J Neurophysiol 94: 295–313, 2005.
First published February 9, 2005; doi:10.1152/jn.01095.2004.

Neurodynamics of Biased Competition and Cooperation for Attention: A Model With Spiking Neurons

Gustavo Deco[1] and Edmund T. Rolls[2]

[1]*Department of Technology, Computational Neuroscience, Institució Catalana de Recerca i Estudis Avançats, Universitat Pompeu Fabra, Barcelona, Spain; and* [2]*Department of Experimental Psychology, University of Oxford, Oxford, United Kingdom*

Submitted 19 October 2004; accepted in final form 27 January 2005

Deco, Gustavo and Edmund T. Rolls. Neurodynamics of biased competition and cooperation for attention: a model with spiking neurons. *J Neurophysiol* 94: 295–313, 2005. First published February 9, 2005; doi:10.1152/jn.01095.2004. Recent neurophysiological experiments have led to a promising "*biased competition hypothesis*" of the neural basis of attention. According to this hypothesis, attention appears as a sometimes nonlinear property that results from a top-down biasing effect that influences the competitive and cooperative interactions that work both within cortical areas and between cortical areas. In this paper we describe a detailed dynamical analysis of the synaptic and neuronal spiking mechanisms underlying biased competition. We perform a detailed analysis of the dynamical capabilities of the system by exploring the stationary attractors in the parameter space by a mean-field reduction *consistent* with the underlying synaptic and spiking dynamics. The nonstationary dynamical behavior, as measured in neuronal recording experiments, is studied by an integrate-and-fire model with realistic dynamics. This elucidates the role of cooperation and competition in the dynamics of biased competition and shows why feedback connections between cortical areas need optimally to be weaker by a factor of about 2.5 than the feedforward connections in an attentional network. We modeled the interaction between top-down attention and bottom-up stimulus contrast effects found neurophysiologically and showed that top-down attentional effects can be explained by external attention inputs biasing neurons to move to different parts of their nonlinear activation functions. Further, it is shown that, although NMDA nonlinear effects may be useful in attention, they are not necessary, with nonlinear effects (which may appear multiplicative) being produced in the way just described.

INTRODUCTION

Cognitive behavior relies on a perceptual system that is able to efficiently select the relevant information to which one reacts. Biological systems use a selection-processing strategy for managing the enormous amount of information resulting from their interaction with the environment. This selection of relevant information is referred to as *attention*. Visual attention is the result of top-down influences on the processing of sensory information in the visual cortex and is thus intrinsically associated with neural interactions within and between cortical areas. Thus elucidating the neural basis of visual attention is an excellent paradigm for understanding the basic mechanisms of cortical neurodynamics.

New observations from a number of cognitive neuroscience experiments led to a promising account of attention termed the "*biased competition hypothesis*, " which aims to explain the computational processes governing visual attention and their implementation in the brain's neural circuits and neural systems. According to this hypothesis, attentional selection operates in parallel by biasing an underlying competitive interaction between multiple stimuli in the visual field toward one stimulus or another, so that behaviorally relevant stimuli are processed in the cortex whereas irrelevant stimuli are filtered out (Chelazzi 1998; Chelazzi et al. 1993; Duncan 1996; Reynolds and Desimone 1999). Thus attending to a stimulus at a particular location or with a particular feature biases the underlying neural competition in a certain brain area in favor of neurons that respond to the location, or the features, of the attended stimulus. This attentional effect is produced by generating signals in areas outside the visual cortex that are then fed back to extrastriate visual cortical areas, where they bias the competition such that when multiple stimuli appear in the visual field, the cells representing the attended stimulus *win*, thereby suppressing the firing of cells representing distracting stimuli (Desimone and Duncan 1995; Duncan 1996; Duncan and Humphreys 1989; Reynolds et al. 1999). According to this line of work, attention appears as a property of competitive/cooperative interactions that work in parallel across the cortical modules. Neurophysiological experiments are consistent with this hypothesis in showing that attention serves to modulate the suppressive interaction between the neuronal firing elicited by 2 or more stimuli within the receptive field (Chelazzi 1998; Miller et al. 1993; Motter 1993; Reynolds and Desimone 1999; Reynolds et al. 1999). Further evidence comes from functional magnetic resonance imaging (fMRI) in humans (Kastner et al. 1998, 1999), which indicates that when multiple stimuli are present simultaneously in the visual field, their cortical representations within the object-recognition pathway interact in a competitive, suppressive fashion, which is not the case when the stimuli are presented sequentially. It was also observed that directing attention to one of the stimuli counteracts the suppressive influence of nearby stimuli.

Neurodynamical models providing a theoretical framework for biased competition have been proposed and successfully applied in the context of attention and working memory. In the context of attention, Usher and Niebur (1996) introduced an early model of biased competition to explain the attentional effects in neural responses observed in the inferotemporal cortex, and this was followed by a model for V2 and V4 by Reynolds et al. (1999) based on the shunting equations of Grossberg (1988). Deco and Zihl (2001) extended Usher and

Address for reprint requests and other correspondence: E. T. Rolls, University of Oxford, Dept. of Experimental Psychology, South Parks Road, Oxford OX1 3UD, UK (E-mail Edmund.Rolls@psy.ox.ac.uk).

The costs of publication of this article were defrayed in part by the payment of page charges. The article must therefore be hereby marked "*advertisement*" in accordance with 18 U.S.C. Section 1734 solely to indicate this fact.

Niebur's model to simulate the psychophysics of visual attention by visual search experiments in humans. Their neurodynamical formulation is a large-scale hierarchical model of the visual cortex whose global dynamics is based on biased-competition mechanisms at the neural level. Attention then appears as an effect related to the dynamical evolution of the whole network. This large-scale formulation has been able to simulate and explain in a unifying framework visual attention in a variety of tasks and at different cognitive neuroscience experimental measurement levels: single cells (Deco and Lee 2002; Rolls and Deco 2002), fMRI (Corchs and Deco 2002, 2004), psychophysics (Deco and Rolls 2004; Deco et al. 2002), and neuropsychology (Deco and Rolls 2002; Heinke et al. 2002). In the context of working memory, further developments (Deco and Rolls 2003; Deco et al. 2004; Szabo et al. 2004) managed to model in a unifying form attentional and memory effects in the prefrontal cortex integrating single-cell and fMRI data, and different paradigms in the framework of biased competition.

In spite of the successful application of the biased-competition principle in large-scale cognitive neuroscience modeling, a detailed dynamical analysis of the underlying synaptic and spiking mechanisms is still missing. The existing models cited above are all based on rate models [apart from the one-layer model of Usher and Niebur (1996), considered further in the DISCUSSION], which simplify and capture the qualitative behavior of the dynamics, but are not quantitatively directly related with the underlying synaptic and spiking neural activity. Moreover, because the biased competition effect is essentially a dynamical effect emerging from a complex system (even in the most simple and minimal case), a mere qualitative description of the dynamics could be very wrong and misleading (e.g., the whole system could show different behavior if the underlying nonlinearity describing the single neurons and their interconnections is wrong or has incorrect time constants and delays). A detailed parameter space exploration of the different dynamical attractors of a neural system, even for the most simple and minimal neural circuit involved in biased competition as set out by Reynolds et al. (1999), is also still missing and could yield extremely relevant information about the role of cooperation mechanisms, the roles of feedforward and feedback interactions between neural layers (with each layer typically a different cortical area in the brain), and the role of the different synaptic components [such as α-amino-3-hydroxy-5-methyl-4-isoxazolepropionic acid (AMPA) vs. *N*-methyl-D-aspartate (NMDA)] in biased competition.

The aim of this paper is to perform a detailed analysis of the synaptic and neural spiking dynamics underlying biased competition. We study a biologically plausible minimal cortical circuit in the framework of the standard biased-competition experiments (Reynolds et al. 1999). We perform a detailed analysis of the dynamical capabilities of the system by exploring the stationary attractors in the parameter space by a mean-field reduction consistent with the underlying synaptic and spiking dynamics. The nonstationary dynamical behavior, for direct comparison with neuronal recording experiments, is studied by a dynamically realistic synaptic and spiking model. This allows us to discover: *1*) the particular role of cooperative and competitive effects in the dynamics of biased competition, *2*) the role of feedforward and feedback interactions between cortical modules, *3*) why the feedback connections are weaker by a factor of about 2.5 than the feedforward connections, and *4*) the role of NMDA synaptic connections for biased competition and attention. Furthermore, we are particularly interested in investigating the interaction between (top-down) attention and (bottom-up) stimulus contrast effects in the light of the recent experimental results obtained by Reynolds and Desimone (2003) and Martinez-Trujillo and Treue (2002). These results were obtained in a paradigm that allowed bottom-up and top-down cortical interactions to be analyzed because both were altered parametrically. A detailed and biologically plausible investigation of the contrast–attention modulation paradigm gives us insight into the implementation of attention, and in particular about whether attention results from an effect caused by an explicitly multiplicative contrast gain modulation effect at the neuronal level [as suggested by Martinez-Trujillo and Treue (2002)], or can be explained just by external biasing synaptic interactions operating on neurons with nonlinear response functions.

METHODS

The experimental protocol

Several experimental results of single-cell recording studies in monkeys are consistent with the biased-competition hypotheses in showing that attention serves to modulate the suppressive interaction between 2 or more stimuli within the receptive field (Chelazzi 1998; Chelazzi et al. 1993; Miller et al. 1993; Moran and Desimone 1985; Motter 1993, 1994; Reynolds and Desimone 1999; Sato 1989; Spitzer et al. 1988). Moran and Desimone (1985) showed that the firing activity of visually tuned neurons in the cortex depended on the location of the target stimulus to which the monkeys were instructed to attend. Based on results of this type, the spatial attentional modulation could be described as a gain change and shifting of V4 receptive fields depending on the locus of attention (Connor et al. 1997; see also Luck et al. 1997 and Reynolds et al. 1999 for V4 and V2).

In particular, we will first concentrate here on the experimental protocol of Reynolds et al. (1999) because they performed single-cell recordings of V2 and V4 neurons in a behavioral paradigm that explicitly separated sensory processing mechanisms from attentional effects, to test the biased-competition hypothesis more directly. They first examined the presence of competitive interactions in the absence of attentional effects within the receptive field by having the monkey attend to a location far outside the receptive field of the neuron that they were recording. They used oriented bars as visual stimuli. They compared the firing activity response of the neuron, when a single reference stimulus was within the receptive field, with the response when a second, "probe," stimulus was added to the field. When the probe was added to the field, the activity of the neuron was shifted toward the activity level that would have been evoked if the probe had appeared alone. When the reference was an effective stimulus (high response) and the probe was an ineffective stimulus (low response), the firing activity was suppressed after adding the probe. On the other hand, the response of the cell increased when an effective probe stimulus was added to an ineffective reference stimulus. Thus the response of a V4 neuron to 2 stimuli in its field is not the sum of its responses to both, but rather is a weighted average of the responses to each stimulus alone. Attentional modulatory effects have been independently tested by repeating the same experiment but now having the monkey attend to the reference stimulus within the receptive field of the recorded neuron. The effect of attention on the response of the V2 or V4 neuron was to almost compensate the suppressive or excitatory effect of the probe. That is, if the probe caused a suppression of the neuronal response to the reference when attention was outside the receptive field, then attending to the reference restored the neuron's

activity to the level corresponding to the response of the neuron to the reference stimulus alone. Symmetrically, if the probe stimulus had increased the neuron's level of activity, attending to the reference stimulus compensated the response by shifting the activity to the level that had been recorded when the reference was presented alone.

In a second step, we will also consider manipulation of the contrast of the visual stimuli as used by Reynolds and Desimone (2003) and Martinez-Trujillo and Treue (2002) to analyze the mutual interaction between top-down attentional effects and (bottom-up) stimulus contrast effects. They used the biased-competition design explained above presenting 2 stimuli (reference and probe) simultaneously. The experiment of Reynolds and Desimone (2003) (again using oriented bars as stimuli) showed that in the absence of attention, increasing the physical contrast of one stimulus caused V4 neurons to respond preferentially to that stimulus, and reduced their responses to the competing stimulus. On the other hand, when attention was directed to the lower-contrast stimulus, it partially overcame the influence of a competing, higher-contrast stimulus. Furthermore, with a similar design, but using middle temporal (MT) neurons and presenting simultaneously both a preferred and a nonpreferred stimulus that consisted of moving dots in a given direction, Martinez-Trujillo and Treue (2002) showed that when attention is directed to the nonpreferred competing stimulus, the response of the neuron decreased with respect to the case when attention was not allocated on either of both stimuli. This attentional effect was maximal at intermediate contrast of the preferred stimulus.

The network model

We analyze the synaptic and spiking mechanisms underlying biased competition for the experimental design described in the previous section by introducing a minimal model of the dynamics between the 2 cortical brain areas involved (see Fig. 1). These 2 cortical areas correspond to V2 and V4 for the Reynolds et al. design (Reynolds and Desimone 2003; Reynolds et al. 1999) and to V1 (or V3) and MT for the Martinez-Trujillo and Treue (2002) design. Both cortical areas have the same internal architecture, and implement a dynamical competition between different neurons. Each cortical area contains N_E (excitatory) pyramidal cells and N_I inhibitory interneurons. In our simulations, we use $N_E = 800$ and $N_I = 200$, consistent with the neurophysiologically observed proportion of 80% pyramidal cells versus 20% interneurons (Abeles 1991; Rolls and Deco 2002). In each cortical area, the neurons are fully connected (with synaptic strengths as specified below). Neurons in each cortical area of the network shown in Fig. 1 are clustered into populations or pools.

There are 2 different types of pool: excitatory and inhibitory; there are 2 subtypes of excitatory pool: specific and nonselective. Specific pools are encoding, for example, the identity of the visual features. Layer V2 (the model of area V2) contains 2 specific pools encoding bar orientation, spatial frequency, and location. We denote these pools $S1$ and $S2$, and consider that each of them has a small nonoverlapping receptive field (i.e., they are sensitive to 2 different locations respectively) and are sensitive to 2 different orientations/spatial frequency, say $O1$ and $O2$, respectively. Layer V4 (the model of area V2) also contains 2 specific pools that we denote $S1'$ and $S2'$. Each of these pools has a larger receptive field that covers the 2 receptive fields considered in layer V2. We consider that the pool $S1'$ has a preferred stimulus, which is the one preferred by the pool $S1$ (i.e., $O1$), and the pool $S2'$ has a preferred stimulus, which is the one preferred by the pool $S2$ (i.e., $O2$). On the other hand, the stimulus $O1$ ($O2$) is a nonpreferred stimulus of $S2'$ ($S1'$). This is implemented by considering that the synaptic feedforward connections J_f and feedback connections J_b between $S1$–$S1'$ and $S2$–$S2'$ are much stronger than the weak synaptic feedforward connections K_f and feedback connections K_b between $S1$–$S2'$ and $S2$–$S1'$. We set $K_f = cJ_f$ and $K_b = cJ_b$, with $c = 0.1$ for the Reynolds et al. (Reynolds and Desimone 2003;

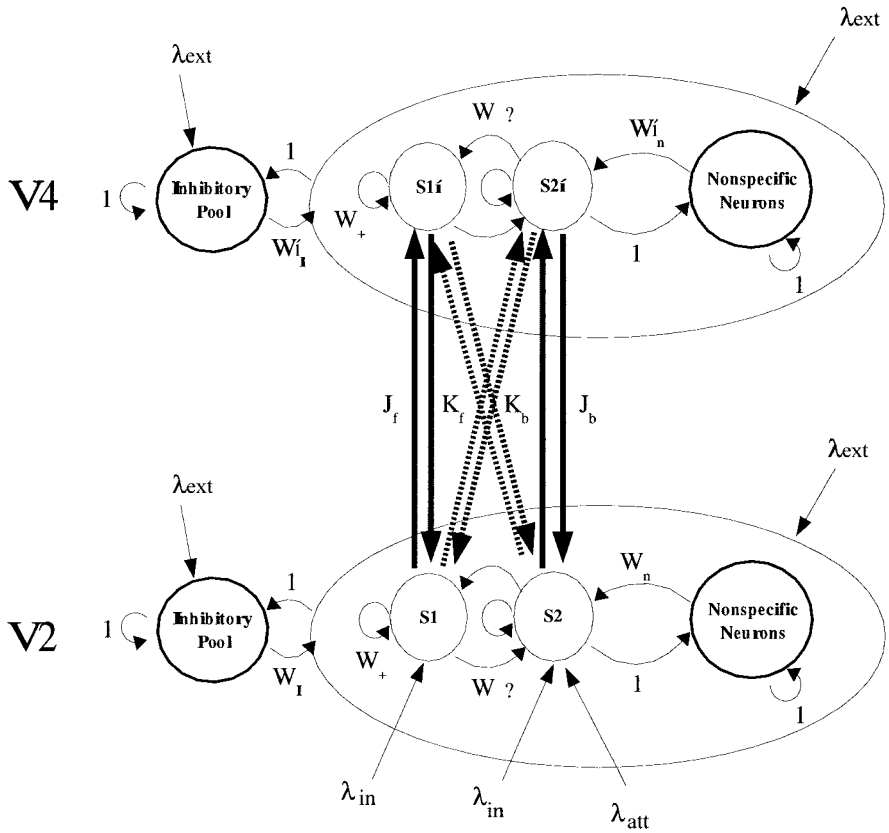

FIG. 1. Minimal model corresponding to the "Biased Competition" experiments of Reynolds et al. (1999). Model considers 2 cortical areas V2 and V4 [or V1 and middle temporal (MT) to model the experiment of Martinez et al. (2002)]. Both cortical areas have the same internal architecture and implement a dynamical competition between different neurons. Each cortical area contains excitatory pyramidal cells and inhibitory interneurons. In each cortical area, the neurons are fully connected (with synaptic strengths as specified in the text). Neurons in each cortical area are clustered into populations or pools. There are 2 different types of pool: excitatory and inhibitory; there are 2 subtypes of excitatory pool: specific and nonselective. Specific pools encode, for example, the visual features that are part of an object. Recurrent arrows indicate recurrent connections between the different neurons in a pool. (See text for more details.)

Reynolds et al. 1999) experiments, and $c = 0.075$ for the Martinez-Trujillo and Treue (2002) experiment. Each specific pool of excitatory cells contains fN_E neurons (in our simulations $f = 0.1$). In both layers, the remaining excitatory neurons do not have specific sensory inputs, and are in a nonselective pool. [They have some spontaneous firing and help to introduce some noise into the simulation, which aids in generating the almost Poisson spike-firing patterns of neurons in the simulation that are a property of many neurons recorded in the brain (Brunel and Wang 2001).] All the inhibitory neurons are clustered into a common inhibitory pool for each module, so that there is global competition throughout each module. We assume that the synaptic coupling strengths between any 2 neurons in the network act as if they were established by Hebbian learning (i.e., the coupling will be strong if the pair of neurons have correlated activity and weak if they are activated in an uncorrelated way). As a consequence of this, neurons within a specific excitatory pool are mutually coupled with a strong weight $w_+ = 1.5$. Neurons in the inhibitory pool are mutually connected with an intermediate weight $w = 1$ [forming the inhibitory-to-inhibitory connections that are useful in achieving nonoscillatory firing (Brunel and Wang 2001)]. They are also connected with all excitatory neurons in the same layer with the same intermediate weight, which for excitatory-to-inhibitory connections is $w = 1$ (in both layers), and for inhibitory-to-excitatory connections is denoted by a weight w_I in layer V2 and w'_I in layer V4.

Because in our model the specific V4 pools have overlapping receptive fields, whereas the specific V2 pools do not have overlapping receptive fields, we consider that the level of competition in V4 is higher than that in V2. This is because the inhibition in both layers is local and therefore the stronger the neighborhood relationship, the stronger the inhibition. Consequently, in topographically organized layers (such as visual cortex layers), the greater degree of overlapping of the receptive fields, the stronger the competition. We thus use in our simulations $w_I = 1$ and $w'_I = 1.25$. The connection strength between 2 neurons in 2 different specific excitatory pools in the same layer is weak and given by $w_- = 1 - f(w_+ - 1)/(1 - f)$, so that the overall recurrent excitatory synaptic drive in the spontaneous state remains constant as w_+ is varied (Brunel and Wang 2001). Neurons in a specific excitatory pool are connected to neurons in the nonselective pool in the same layer with a feedforward synaptic weight $w = 1$ and a feedback synaptic connection of weight $w_n = (-fJ_b - fK_b)/(1 - 2f) + w_-$ in layer V4 and $w'_n = (-fJ_f - fK_f)/(1 - 2f) + w_-$ in layer V2, and these connections normalize each layer so that the overall recurrent excitatory synaptic drive in the spontaneous state remains constant as the external cortical connections J_f, J_b, K_f, and K_b are varied.

Each neuron (pyramidal cells and interneurons) receives $N_{ext} = 800$ excitatory AMPA synaptic connections from outside the network. The external inputs are given by a Poisson train of spikes. To model the background spontaneous activity of neurons in the network (Brunel and Wang 2001), we assume that Poisson spikes arrive at each external synapse with a rate of 3 Hz, consistent with the spontaneous activity observed in the cerebral cortex (Rolls and Treves 1998; Wilson et al. 1994). In other words, the effective external spontaneous background input rate of spikes across the relevant synapses to each cell is $\boldsymbol{\nu}_{ext} = N_{ext} \times 3$ Hz $= 2.4$ kHz. The presentation of a stimulus is simulated by selectively increasing the external rates afferent to the corresponding specific population in layer V2, $\boldsymbol{\nu}_{ext} = \boldsymbol{\nu}_{ext} + \boldsymbol{\lambda}_{in}$. In our experiments, both $S1$ and $S2$ pools in V2 were simultaneously exposed to a stimulus. Attentional biasing is also simulated by selectively increasing the external rates afferent to the corresponding specific population, $\boldsymbol{\nu}_{ext} = \boldsymbol{\nu}_{ext} + \boldsymbol{\lambda}_{att}$, in layer V2 for spatial attention and in layer V4 for object attention. In our simulations we use $\boldsymbol{\lambda}_{in} =$ 250 Hz and $\boldsymbol{\lambda}_{att} = 10$ Hz.

This cortical architecture implements competition within each cortical layer. In each layer, the competition is biased by the external inputs that could originate either from the external visual stimuli presented (to V2) or from attention. The competition in both layers is also mutually biased by the excitatory connections between brain areas. The whole system is therefore a dynamical system with a complex dynamics resulting from local competition mechanisms at each layer and cooperative mechanisms between cortical layers. A thorough analysis thus requires a biologically plausible implementation of the underlying synaptic and neural mechanisms, incorporating the realistic nonlinearities, and synaptic and membrane time constants. The question now is how to implement this, and which methodology to use to analyze the complex dynamics, to extract the conditions for having a combination of cooperative and competitive neural and synaptic mechanisms so that whole dynamics behaves in the same way as is found in the neurophysiological results.

The synaptic and spiking mechanisms

We assume that a proper level of description at the microscopic level is captured by the spiking and synaptic dynamics of one-compartment, pointlike models of neurons, such as *integrate-and-fire* models. The realistic dynamics allows the use of realistic biophysical constants (such as conductances, delays, etc.) in a thorough study of the realistic timescales and firing rates involved in the evolution of the neural activity underlying cognitive processes, for comparison with experimental data. We believe that it is essential of a *biologically plausible* model that the different timescales involved are properly described because the system that we are describing is a dynamical system that is sensitive to the underlying different spiking and synaptic time courses, and the nonlinearities involved in these processes. For this reason, it is convenient to include a thorough description of the different time courses of the synaptic activity, by including fast and slow excitatory receptors (AMPA and NMDA) and $\boldsymbol{\gamma}$-aminobutyric acid (GABA)–inhibitory receptors.

An integrate-and-fire neuron can be described by a basic circuit consisting of a capacitance (the cell membrane capacitance C_m) in parallel with a resistance (the cell membrane resistance R_m) driven by input currents coming from connected neurons. When the voltage across the membrane capacitance reaches a given threshold the circuit is shunted and the neuron generates a spike that is then transmitted to other neurons. The spikes arriving to a given neuron produce postsynaptic excitatory or inhibitory potentials (basically through a low-pass filter formed by the synaptic and membrane time constants) and constitute the incoming input to the neuron. We also include spike-frequency–adapting mechanisms, by Ca^{2+}-activated K^+ hyperpolarizing currents (Liu and Wang 2001), but these are for biophysical realism and to make the time courses shown similar to those measured neurophysiologically, and are not essential to any of the effects described. In the integrate-and-fire neuronal model used the recurrent excitatory postsynaptic currents have 2 components: a fast one mediated by AMPA receptors and a slow one mediated by NMDA receptors. We consider that the NMDA currents have a voltage dependency that is controlled by the extracellular magnesium concentration (Jahr and Stevens 1990). The inputs from neurons not explicitly modeled in the network considered are mediated by AMPA receptors. The inhibitory currents into both excitatory and inhibitory cells are GABAergic. The mathematical formulation of the integrate-and-fire neurons and synaptic currents as well as the values of the constants used are given in APPENDIX A.

Stationary and nonstationary dynamics

The simulation of a network of integrate-and-fire neurons allows the study of the dynamical behavior of the neuronal spiking rates. However, these simulations are computationally expensive and their results probabilistic, which makes them rather unsuitable for systematic parameter explorations. The standard strategy to solve this problem is to simplify the dynamics by the *mean-field* approach at least for the stationary conditions (i.e., for periods after the dynamical tran-

sients) and to analyze there the different dynamical states. The essence of the mean-field approximation is to simplify the integrate-and-fire equations by replacing, after the diffusion approximation (Tuckwell 1988), the sums of the synaptic components by the average DC component and a fluctuation term. The stationary dynamics of each population can be described by the *population transfer function*, which provides the average population rate as a function of the average input current. The set of stationary, self-reproducing rates $\boldsymbol{\nu}_i$ for the different populations i in the network can be found by solving a set of coupled self-consistency equations. This enables a posteriori selection of the parameter region that shows in the dynamics the behavior that we are looking for (e.g., biased competition).

After that, with this set of parameters, we perform the full nonstationary simulations using the *true dynamics* described only by the full integrate-and-fire scheme. The mean-field study ensures that the dynamics will converge to a stationary attractor that is consistent with what we were looking for (Brunel and Wang 2001; Del Giudice et al. 2003). Therefore we used a mean-field approximation to explore how the different operational regimes of the network depend on the values of certain parameters. The mean-field analysis performed in this work uses the formulation derived by Brunel and Wang (2001), which is consistent with the network of neurons used. Their formulation departs from the equations describing the dynamics of one neuron to reach a stochastic analysis of the mean first-passage time of the membrane potentials, which results in a description of the population spiking rates as functions of the model parameters. The mathematical framework is summarized in APPENDIX B.

RESULTS

Standard biased competition design

We consider first a detailed parameter analysis of the possible stationary states of a simplified model of the attentional effects on competing visual stimuli as found by Reynolds et al. (1999) and Reynolds and Desimone (1999). For this we use the consistent mean-field approximation described in the preceding section and in APPENDIX B. We explore the behavior of the network as a function of the feedforward and feedback synaptic connections between the 2 cortical brain areas described in the model (i.e., as a function of J_f and J_b). With this analysis we aim to characterize the different modes of operation of the network and their robustness, which arise from the complex dynamical interplay between the 2 cortical modules, with cooperation between cortical areas and competition within a cortical area mutually biasing each other.

In the standard experimental design both stimuli are presented simultaneously. We consider this by externally and simultaneously exciting the 2 specific pools $S1$ and $S2$. This is done by selectively increasing the external rates afferent to both specific pools $S1$ and $S2$ in layer V2, i.e., $\boldsymbol{\nu}_{\text{ext}}^{S1} = \boldsymbol{\nu}_{\text{ext}}^{S1} + \boldsymbol{\lambda}_{\text{in}}$ and $\boldsymbol{\nu}_{\text{ext}}^{S2} = \boldsymbol{\nu}_{\text{ext}}^{S2} + \boldsymbol{\lambda}_{\text{in}}$. (The supraindex denotes the name of the pool.) Let us denote with $\boldsymbol{\nu}_{\text{Si}}^{\text{noatt}}$ the stationary values of the averaged population activity in pool Si under this condition of simultaneous presentation of both visual stimuli in the absence of attention. To examine the effects of attention across neurons, the experimental work computed a change measurement M, in which the difference between the attended (att) and not-attended (noatt) responses is scaled by the size of the not-attended responses. If spatial attention is allocated to the preferred stimulus, the neural activity is enhanced. On the other hand, if spatial attention is allocated to the nonpreferred stimulus the neural activation is partially suppressed. To consider both effects, we computed the same attentional change measurement M on all 4 specific pools in both cortical modules. For this, we also consider the stationary values of the averaged population activity in all specific pools under the condition where spatial attention is allocated to the location corresponding to the stimulus associated with the pool $S1$ and both stimuli are simultaneously presented. This is done by selectively increasing the external rates afferent to specific pool $S1$, taking into account the external stimulus and the extra external attentional bias (i.e., $\boldsymbol{\nu}_{\text{ext}}^{S1} = \boldsymbol{\nu}_{\text{ext}}^{S1} + \boldsymbol{\lambda}_{\text{in}} + \boldsymbol{\lambda}_{\text{att}}$) and increasing the external rates afferent to specific pool $S2$, taking into account only the presence of the external stimulus (i.e., $\boldsymbol{\nu}_{\text{ext}}^{S2} = \boldsymbol{\nu}_{\text{ext}}^{S2} + \boldsymbol{\lambda}_{\text{in}}$). Let us denote with $\boldsymbol{\nu}_{\text{Si}}^{\text{att}}$ the stationary values of the averaged population activity in pool Si under this condition of simultaneous presentation of both visual stimuli, with spatial attention allocated to stimulus $S1$. The enhancement effect of attention on the activity of pools $S1$ in V2 and $S1'$ in V4 is then given by

$$M^{S1} = \frac{\boldsymbol{\nu}_{S1}^{\text{att}} - \boldsymbol{\nu}_{S1}^{\text{noatt}}}{\boldsymbol{\nu}_{S1}^{\text{noatt}}}$$

$$\mathrm{M}^{S1'} = \frac{\boldsymbol{\nu}_{S1'}^{\text{att}} - \boldsymbol{\nu}_{S1'}^{\text{noatt}}}{\boldsymbol{\nu}_{S1'}^{\text{noatt}}}$$

respectively. The suppressive effect of attention on the activity of pools $S2$ in V2 and $S2'$ in V4 is given by

$$M^{S2} = \frac{\boldsymbol{\nu}_{S2}^{\text{noatt}} - \boldsymbol{\nu}_{S2}^{\text{att}}}{\boldsymbol{\nu}_{S2}^{\text{noatt}}}$$

$$\mathrm{M}^{S2'} = \frac{\boldsymbol{\nu}_{S2'}^{\text{noatt}} - \boldsymbol{\nu}_{S2'}^{\text{att}}}{\boldsymbol{\nu}_{S2'}^{\text{noatt}}}$$

respectively.

The experimental values reported for attentional enhancement modulation in V2 are about 10% and in V4 about 30% (Reynolds et al. 1999). On the other hand, the experimental values reported for attentional suppressive modulation are in V2 about 8%, and in V4 about 25% (Reynolds and Desimone 1999, 2003; Reynolds et al. 1999). To consider all attentional effects in one measure M^{BC}, we define a modulation index that incorporates all these experimental quantitative values into one, which is given by

$$M^{\text{BC}} = 1 - \frac{\left[\left|\frac{M^{S1} - 0.1}{0.1}\right| + \left|\frac{M^{S1'} - 0.3}{0.3}\right| + \left|\frac{M^{S2} - 0.08}{0.08}\right| + \left|\frac{M^{S2'} - 0.25}{0.25}\right|\right]}{4}$$

The modulation index M^{BC} takes into account quantitatively all up-regulating and down-regulating attentional effects as observed in the experiments, and is thus a sensitive measure of the underlying competitive and cooperative dynamics that cause it. Values of M^{BC} close to 1 mean a suitable fit with the quantitative attentional modulation values observed in the experiments under all stimulation conditions and in both the V2 and V4 layers.

Figure 2 shows the parameter exploration for the connection strengths between cortical areas plotting the attentional modulation measure M^{BC} for the stationary states as a function of the feedforward and feedback V2–V4 synaptic connections J_f and J_b. Figure 2*A* shows a 3-dimensional (3D) plot that reflects a narrow parameter region where a delicate dynamical equilibrium between intracortical competition (in each layer) and mutual cooperation between cortical areas yields biased com-

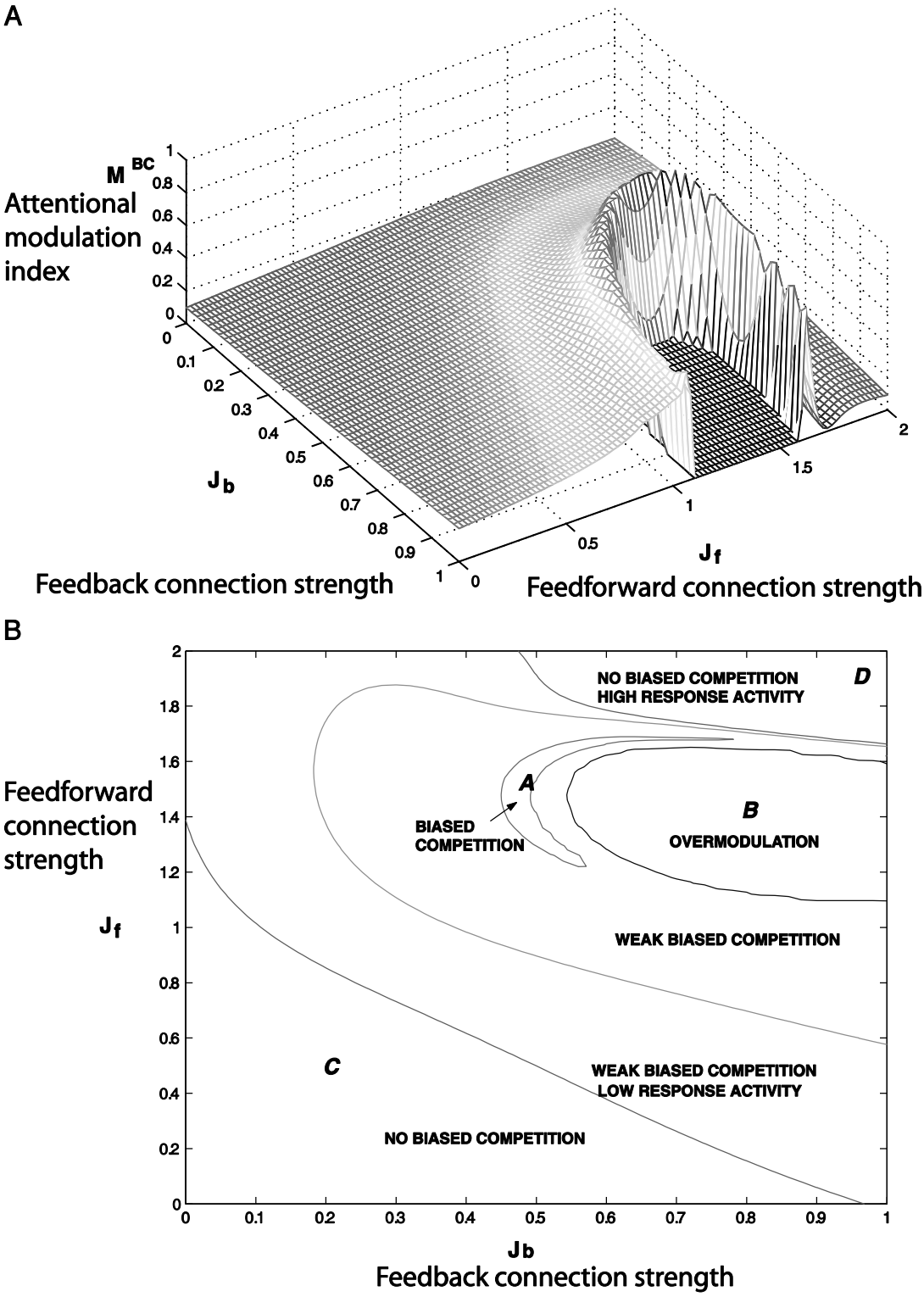

FIG. 2. Interarea cortical parameter exploration plotting the attentional modulation measure M^{BC} for the stationary states as a function of the feedforward and feedback V2–V4 synaptic connections J_f and J_b. *A*: 3D plot that reveals a narrow parameter region where a delicate dynamical equilibrium between intracortical competition (in each layer) and their mutual interarea cortical cooperation yields biased competition similar to that found in the neurophysiological experiments. *B*: 2D projection where the different stationary dynamical regions for the other parameter regions are characterized.

petition according to the quantitative experimental observation. This narrow region, where M^{BC} is close to 1, is around the point "A" where the optimal value of M^{BC} is with $J_f = 1.5$ and $J_b = 0.6$. This result allows us to conclude 2 important facts. First, the region of the parameter space for the connection strengths between cortical areas where the system shows biased competition according to the experimental modulation and response values is very narrow. This implies a delicate dynamical interplay between interarea cortical cooperation and intraarea cortical competition. Second, these results show that

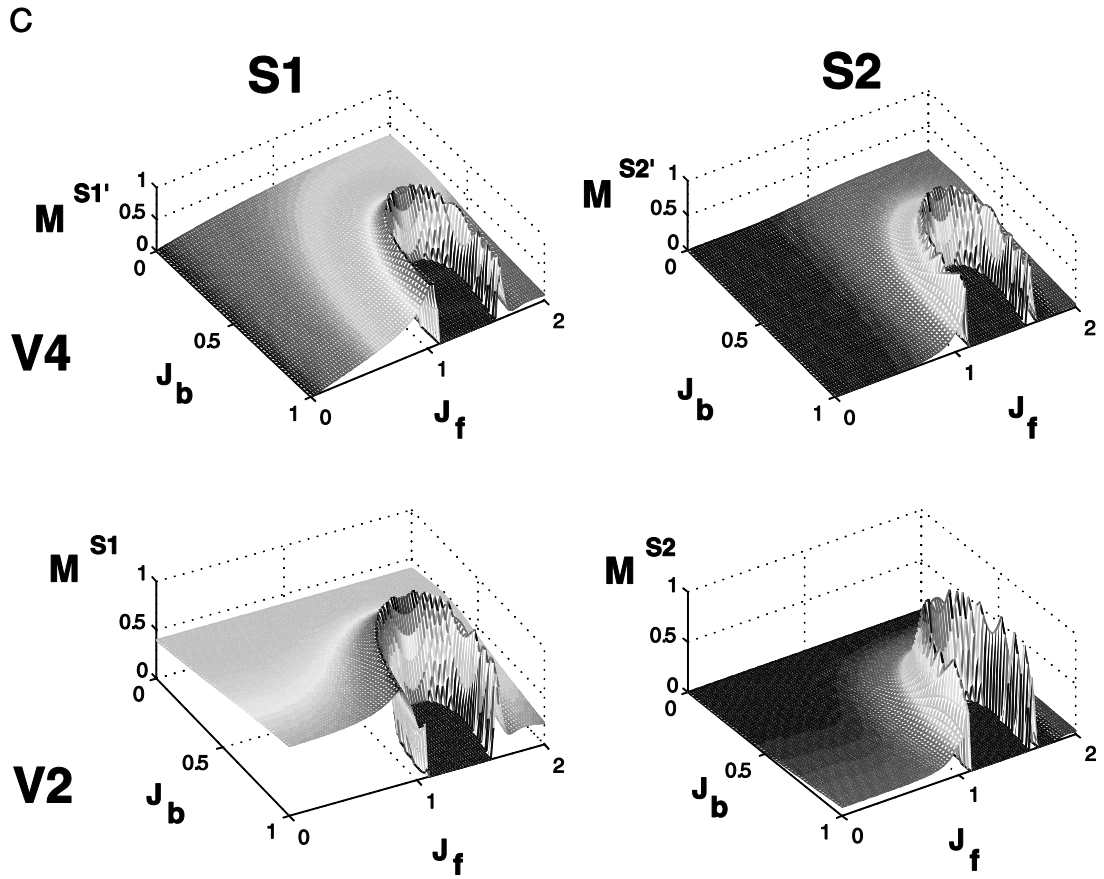

FIG. 2. (*continued*) *C*: attentional modulation measure *M* plotted separately for V4 (*top*, indicated by a ′) and for V2 (*bottom*), for both the neuronal pools selective for *S*1 (*left*) and for *S*2 (*right*) (see RESULTS for definitions). Plotting conventions are as for Fig. 2 *A*, which shows M^{BC}, but in *C* the components of M^{BC} are shown separately.

the feedback interarea cortical interactions (at least in the visual cortex) must for optimal performance be weaker (by a factor of about 1.5/0.6 = 2.5) than the feedforward connections, which is a frequent assumption in the neurophysiological literature but not based on quantitative analysis of the dynamics. Moreover, it is with this ratio for feedforward strength/top-down strength of about 2.5 that the interaction effects between top-down attention and bottom-up contrast changes are found (described in the next section).

Figure 2*B* shows a 2-dimensional (2D) projection where the different stationary dynamical regions for the other parameter regions are characterized. The dividing lines between the regions are set by choosing values for M^{BC} that divide the space into regions that operate qualitatively differently. The region at the *top* around the point "D" (high J_f and high J_b) corresponds to a region that we call "No Biased Competition: High Response Activity" because there is low attentional modulation (both up-regulating and down-regulating), and relatively high neural responses in both specific pools of areas V2 and V4. The region around point "B," which has higher feedback values as required for biased competition, corresponds to a dynamical attractor that we call "Overmodulation" because the attentional modulation effects are unrealistically high, in spite of the fact that the level of response activity in the absence of attention is in the experimental range. There are large regions of the parameter space that we characterize as "Weak Biased Competition," corresponding to a dynamical attractor that shows attentional modulation qualitatively according to biased competition but quantitatively too weak, and with the normal level of neural response when attention is absent. This region is followed by another region "Weak Biased Competition: Low Activity Response," which also shows a low level of neural response in the absence of attention. The last region, corresponding to low feedforward values and called "No Biased Competition," shows a low level of response with no attentional modulation.

Figure 2*C* shows the attentional modulation measure *M* plotted separately for V4 (*top*, indicated by a ′) and for V2 (*bottom*), for both the neuronal pools selective for *S*1 (*left*) and for *S*2 (*right*) (see RESULTS for definitions). Figure 2*C* thus shows the 4 components of M^{BC}, as defined above, and shows that attentional enhancement is largely restricted to a C-shaped region in which the feedforward connection strength is nearly twice the feedback connection strength. At those values, for our modeled neurons responding to stimulus 1, we see that there is up to a 30% increase in the responses of V2 cells and up to a 25% increase in the responses of V4 cells, consistent with reported attentional effects. Figure 2*C* thus confirms that the attentional modulation is operating correctly in both V4 and V2, and for both the neuronal populations selective to *S*1 and those selective to *S*2. The attentional modulation is qualitatively similar in V4 and V2, consistent with the fact that both areas operate with internal competition, which is influenced by both bottom-up and top-down external inputs.

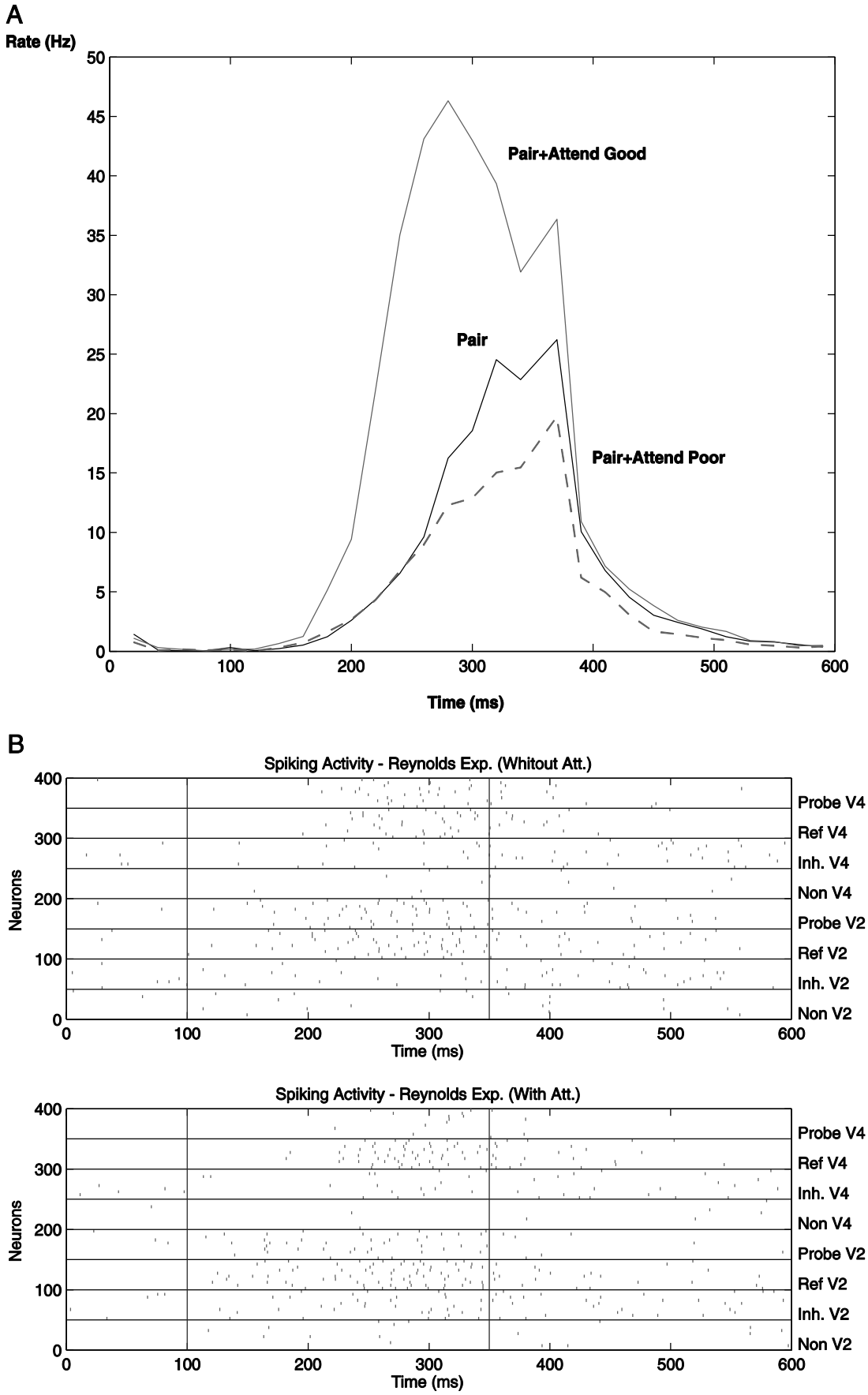
A
Rate (Hz)
Pair+Attend Good
Pair
Pair+Attend Poor
Time (ms)
B
Spiking Activity - Reynolds Exp. (Whitout Att.)
Neurons
Probe V4
Ref V4
Inh. V4
Non V4
Probe V2
Ref V2
Inh. V2
Non V2
Time (ms)
Spiking Activity - Reynolds Exp. (With Att.)
Neurons
Probe V4
Ref V4
Inh. V4
Non V4
Probe V2
Ref V2
Inh. V2
Non V2
Time (ms)

Figure 3 shows the nonstationary behavior of the neurodynamical activity in the full spiking and synaptic simulation of the network for the particular point "A" of the region showing biased competition. The simulation corresponds to the experimental design of Reynolds et al. (Reynolds and Desimone 1999; Reynolds et al. 1999). After a period of spontaneous activity of 100 ms without stimulation, the stimuli are presented for 250 ms. After that the stimuli disappear again and a period of 250 ms is shown. Figure 3*A* plots the development of the firing rate activity for V4 specific neurons tuned to the preferred stimulus showing that the attended stimulus controls the response of the neuron. The rates were calculated by averaging the responses over 20 trials of all the neurons (80) in the pool of specific V4 neurons responding to the preferred stimulus. The line in the *middle* shows the response when the 2 stimuli are shown, a preferred (good or effective) stimulus and a nonpreferred (poor) stimulus, with attention directed away from the receptive field ("Pair" condition). The line at the *top* shows the response when the 2 stimuli are presented together, with attention directed to the good stimulus ("Pair+Attend Good" condition). An attentional enhancement is observed. The line at the *bottom* shows the response when the 2 stimuli are presented together, with attention directed to the poor stimulus ("Pair+Attend Poor" condition). An attentional suppression is observed. Figure 3*B* plots the rastergrams of randomly selected neurons for each pool in the network (5 neurons for each pool). Two conditions are shown: the Pair condition (Without Attention) and Pair+Attend Good condition (With Attention). The spatiotemporal spiking activity shows the up-regulation of the spiking activity in the V2 and V4 neurons whose preferred stimulus (labeled Ref) is attended, and also simultaneously the down-regulation of spiking activity in the V2 and V4 neurons whose nonpreferred stimulus (labeled Probe) is attended (see Fig. 3*B*). The corresponding plots for the nonstationary behavior of the neurodynamical activity of the network for the particular point "C" of the region showing no biased competition are shown in Fig. 4.

Attentional modulation and stimulus contrast

To investigate the interactions between bottom-up visual salience information (such as that influenced by stimulus contrast) and attentional top-down information, Reynolds and Desimone (2003) and Martinez-Trujillo and Treue (2002) performed variations of the standard biased-competition design by manipulating the contrast of one of the competing stimuli, as described above (see METHODS). The special relationship found in the neurophysiological experiments between contrast and attention suggested (Martinez-Trujillo and Treue 2002) that attention provokes a multiplicative change of the neural contrast gain [see Figs. 1 and 3 of Reynolds and Desimone (2003)]. To understand the interactions found, we simulated both experiments as follows.

The design of the experiments and the different measures as implemented in our simulations are shown graphically in Fig. 5. Figure 5*A* shows the design of Reynolds and Desimone (2003). They measured the neuronal response in V4, manipulating the contrast of the nonpreferred stimulus and comparing the response to both stimuli when attention was allocated to the poor stimulus. They observed that the attentional suppressive effect of the competing nonpreferred stimulus is higher when the contrast of that stimulus increases. In our simulations we measured neuronal responses from neurons in pool $S1'$ in V4 to both preferred and nonpreferred stimuli simultaneously presented within the receptive field. We manipulated the contrast of the stimulus that was nonpreferred for the neurons $S1'$ (in the simulation by altering $\boldsymbol{\lambda}_{\text{in}}$ to $S2$). We analyzed the effects of this manipulation for 2 conditions: without spatial attention or with spatial attention on the nonpreferred stimulus $S2$, implemented by adding an extra bias $\boldsymbol{\lambda}_{\text{att}}$ to $S2$.

Figure 6 (*top*) shows the results of our simulations for the design of Reynolds and Desimone (2003). We observed that the attentional suppressive effect implemented through $\boldsymbol{\lambda}_{\text{att}}$ on the responses of neurons $S1'$ of the competing nonpreferred stimulus is higher when the contrast of the nonpreferred stimulus increases, as in the original neurophysiological experiments. The *top* figure shows the response of a V4 neuron to different log contrast levels (abscissa) in the no-attention condition (AO: attending outside the receptive field) and in the attention condition (AI: attending inside the receptive field). The *top right* part of Fig. 6 shows the difference between both conditions. As in the experimental observations the suppressive effect of the competing nonpreferred stimulus is higher when the contrast of that stimulus increases but, at higher levels of salience (contrast), the top-down attentional effect disappears.

To study the relevance of NMDA synapses for the interarea cortical dynamics of attention, we repeated the analysis shown in Fig. 6 (*top*), but with the voltage-dependent nonlinearity removed from the NMDA receptors (in the feedforward, the feedback, and the recurrent collateral connections) by setting $Mg^{2+} = 0$ (which corresponds to removing the nonlinear dependency of the NMDA synapses on the postsynaptic potential, as shown in APPENDIX A). [We compensated for the

FIG. 3. Nonstationary behavior of the neurodynamical activity performed by the full spiking and synaptic simulation of the network for the particular point "A" of the region showing biased competition. Simulation corresponds to the experimental design of Reynolds et al. (1999). *A*: plots the development of the firing rate for selective V4 neurons to one good or preferred stimulus and one poor (nonpreferred) stimulus presented simultaneously, both within the receptive field. Stimuli were ON in the period 100–350 ms. Figure shows that attention controls the response of the neuron, as follows. *Middle line*: response when attention is directed away from the receptive field of the neuron ("Pair" condition, also termed a "Without Attention" condition). *Top line*: response with attention directed to the good (or preferred) stimulus ("Pair+Attend Good" condition). An attentional enhancement is observed. *Bottom line*: response when attention is directed to the poor stimulus ("Pair+Attend Poor" condition). An attentional suppression is observed. *B*: plots the poststimulus rastergrams of randomly selected neurons for each pool in the network (with 5 neurons shown from each pool). Each small vertical line is the spike from a neuron, and each row shows the spikes of one neuron. Stimuli were ON in the period 100–350 ms. Two conditions are shown. In the *bottom panel* (With attention) the firing of neurons tuned to the preferred stimulus (labeled Ref, signifying the reference stimulus) is enhanced when attention is directed to this stimulus. At the same time (i.e., with attention to the Ref stimulus), the response of other neurons whose preferred stimulus is the Probe is down-regulated. *Top panel* (Without attention): responses of both sets of neurons (Ref and Probe) to the pair stimuli when attention is directed outside the receptive field, providing the baseline condition against which the up-regulation or down-regulation in the *bottom panel* is measured. Labels indicate the different pools, with "Probe V4" the pool of neurons in V4 tuned to the Probe stimulus, "Ref V2" the pool of neurons in V2 tuned to the Reference stimulus, "Non V2" the pool of neurons in V2 with nonspecific activity (i.e., not tuned to either of the stimuli), and "Inh V2" the pool of inhibitory neurons in V2, and so forth.

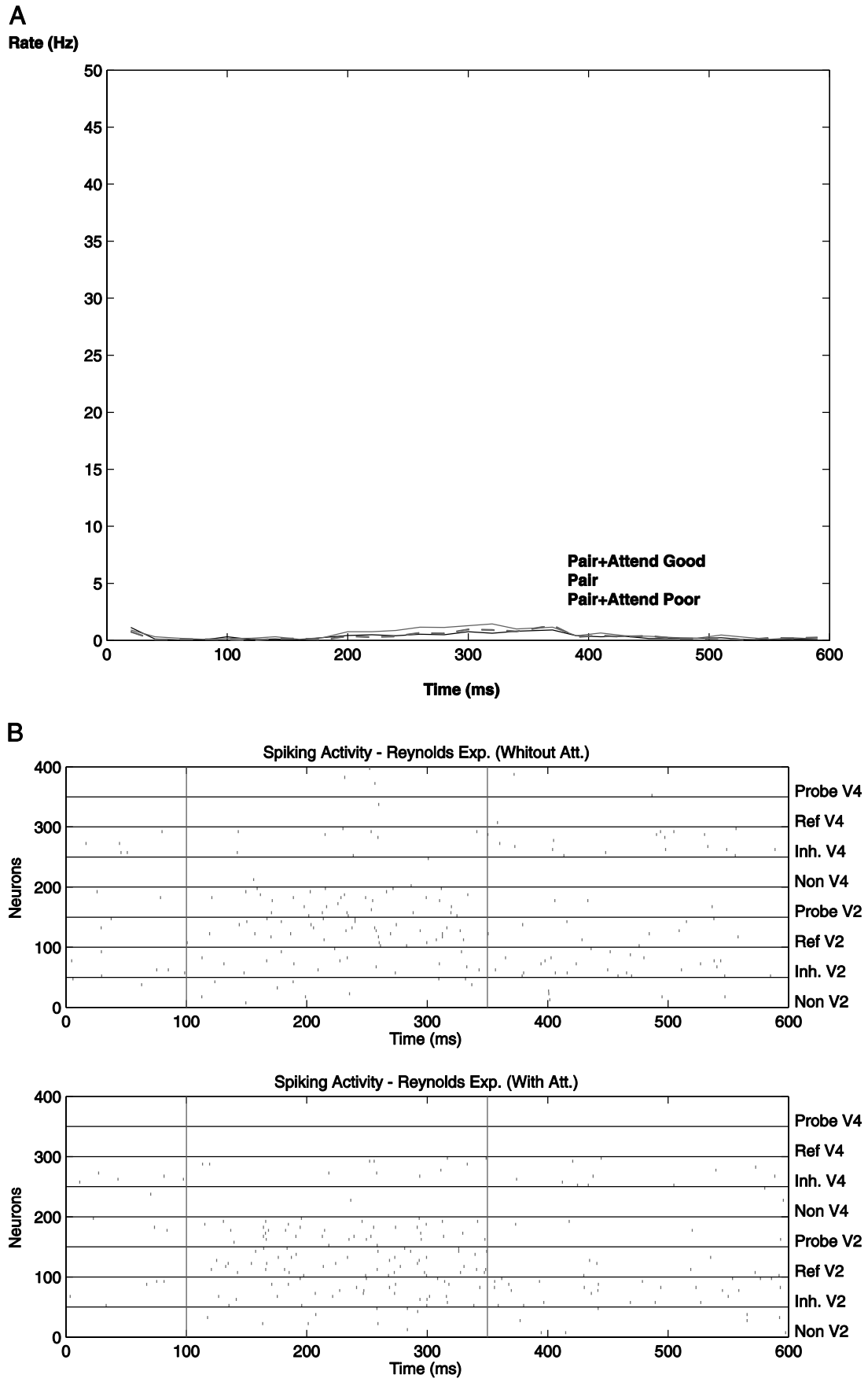

FIG. 4. Same plots as in Fig. 3, but corresponding to the nonstationary behavior of the neurodynamical activity of the network for the particular point "C" of the region in Fig. 2*B* showing no biased competition.

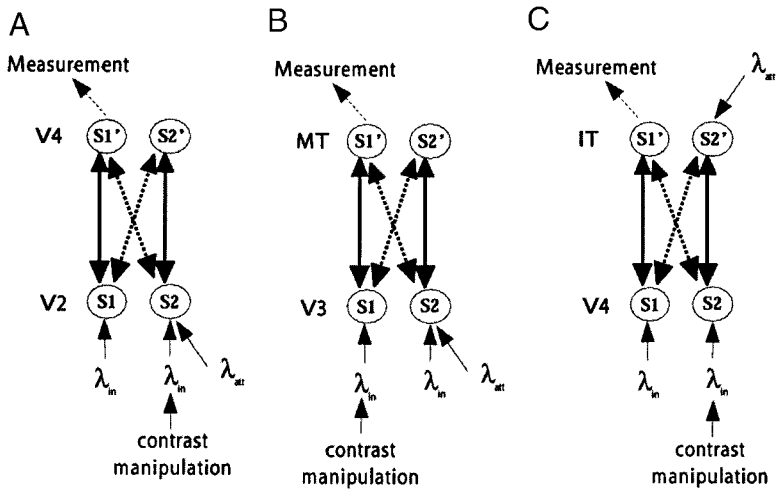

FIG. 5. Interaction between salience (contrast, a bottom-up influence) and attention (a top-down influence) in 2 different biased competition designs. *A*: design of Reynolds and Desimone (2003) as implemented in the simulations. We measured neuronal responses from neurons in pool $S1'$ in V4 to a preferred and a nonpreferred stimulus simultaneously presented within the receptive field. We manipulated the contrast of the stimulus that was nonpreferred for the neurons $S1'$ (in the simulation by altering $\boldsymbol{\lambda}_{in}$ to $S2$). We analyzed the effects of this manipulation for 2 conditions: without spatial attention or with spatial attention on the nonpreferred stimulus $S2$, implemented by adding an extra bias $\boldsymbol{\lambda}_{att}$ to $S2$. We observed that the attentional suppressive effect implemented through $\boldsymbol{\lambda}_{att}$ on the responses of neurons $S1'$ of the competing nonpreferred stimulus is higher when the contrast of the nonpreferred stimulus increases, as in the original neurophysiological experiments. *B*: implementation in the simulation of the design of Martinez and Treue (2002). We measured neuronal responses in MT from neurons $S1'$ to 2 moving patterns, manipulating the contrast of the preferred stimulus (for neurons $S1$) and comparing the response from neurons $S1'$ when spatial attention was allocated to the competing nonpreferred stimulus implemented by adding $\boldsymbol{\lambda}_{att}$ to alter the responses of neurons $S2$. We observed that the attentional suppressive effect implemented through $\boldsymbol{\lambda}_{att}$ of the competing nonpreferred stimulus is higher when the contrast of the preferred stimulus is at intermediate values, as in the original neurophysiological experiments. *C*: design associated with a prediction that can be made by setting the contrast–attention interaction study in the framework of the experimental biased competition design of Chelazzi et al. (1993) involving object attention instead of spatial attention. We measured neuronal responses from neurons in pool $S1'$ in IT (inferior temporal cortex) to a preferred and a nonpreferred stimulus simultaneously presented within the receptive field. We manipulated the contrast of the stimulus that was nonpreferred for the neurons $S1'$ (in the simulation by altering $\boldsymbol{\lambda}_{in}$ to $S2$). We analyzed the effects of this manipulation for 2 conditions: without object attention or with top-down object attention on the nonpreferred stimulus $S2'$, implemented by adding an extra bias $\boldsymbol{\lambda}_{att}$ to $S2'$. Results of the simulation lead to the prediction that the attentional suppressive effect implemented through $\boldsymbol{\lambda}_{att}$ on the responses of neurons $S1'$ of the competing nonpreferred stimulus ($S2$) is higher when the contrast of the nonpreferred stimulus ($S2$) is at intermediate values.

effective change of synaptic strength by rerunning the mean-field analysis to obtain the optimal parameters for the simulation (with $M^{BC} = 1$), which was produced with $J_f = 1.6$ and $J_b = 0.42$, and then with these values, we reran the simulation.] The results are shown in Fig. 6 (*middle*), where it is clear that the same attentional effects can be found exactly in the same qualitative and even quantitative form as when the nonlinear property of NMDA receptors is operating. The implication is that the nonlinearity of the effective activation function (firing rate as a function of input current to a neuron) of the neurons (both the threshold and its steeply rising initial part) implicit in the integrate-and-fire model with AMPA and other receptors is sufficient to enable nonlinear attentional interaction effects with bottom-up inputs to be produced. The nonlinearity of the NMDA receptor may facilitate this process by its nonlinearity, but is not necessary.

We further studied the relevance of the NMDA receptors by repeating the analysis in Fig. 6 (*top*), but with the time constants of the NMDA receptors set to be the same values as those of the AMPA receptors [and as in Fig. 6 (*middle*) with the NMDA voltage-dependent effects disabled by setting $Mg^{2+} = 0$]. (We again compensated for the effective change of synaptic strength by rerunning the mean-field analysis to obtain the optimal parameters for the simulation.) The results are shown in Fig. 6 (*bottom*), where it is shown that top-down attentional effects are now substantially reduced. [That is, there is very little difference between the no-attention condition (AO: attending outside the receptive field), and the attention condition (AI: attending inside the receptive field).] This effect is not just because the NMDA receptor system with its long time constant may play a generic role in the operation of the integrate-and-fire system, by facilitating stability and helping to prevent oscillations, because a similar failure of attention to operate normally was also found with the mean-field approach, in which the stability of the system is not an issue. Thus the long time constant of NMDA receptors does appear to be an important factor in enabling top-down attentional processes to modulate correctly the bottom-up effects to account for the effects of attention on neuronal activity. This is an interesting result that deserves further analysis. The mean-field *Eq. B2* of APPENDIX B effectively defines the nonlinear transfer function of the neurons, and this will be affected by the long time constant of the NMDA receptors, as can be seen in the preceding equations of APPENDIX B.

Figure 5*B* shows the design of Martinez-Trujillo and Treue (2002). They measured the neuronal response in MT, manipulating the contrast of the preferred stimulus and comparing the response when attention was allocated on that competing nonpreferred stimulus. They observed that the attentional suppressive effect of the competing nonpreferred stimulus is higher when the contrast of the preferred stimulus is at intermediate values. In our simulations we measured neuronal responses in MT from neurons $S1'$ to 2 moving patterns, manipulating the contrast of the preferred stimulus (for neurons $S1$), and comparing the response from neurons $S1'$ when spatial attention was allocated to the competing nonpreferred stimulus implemented by adding $\boldsymbol{\lambda}_{att}$ to alter the responses of neurons $S2$.

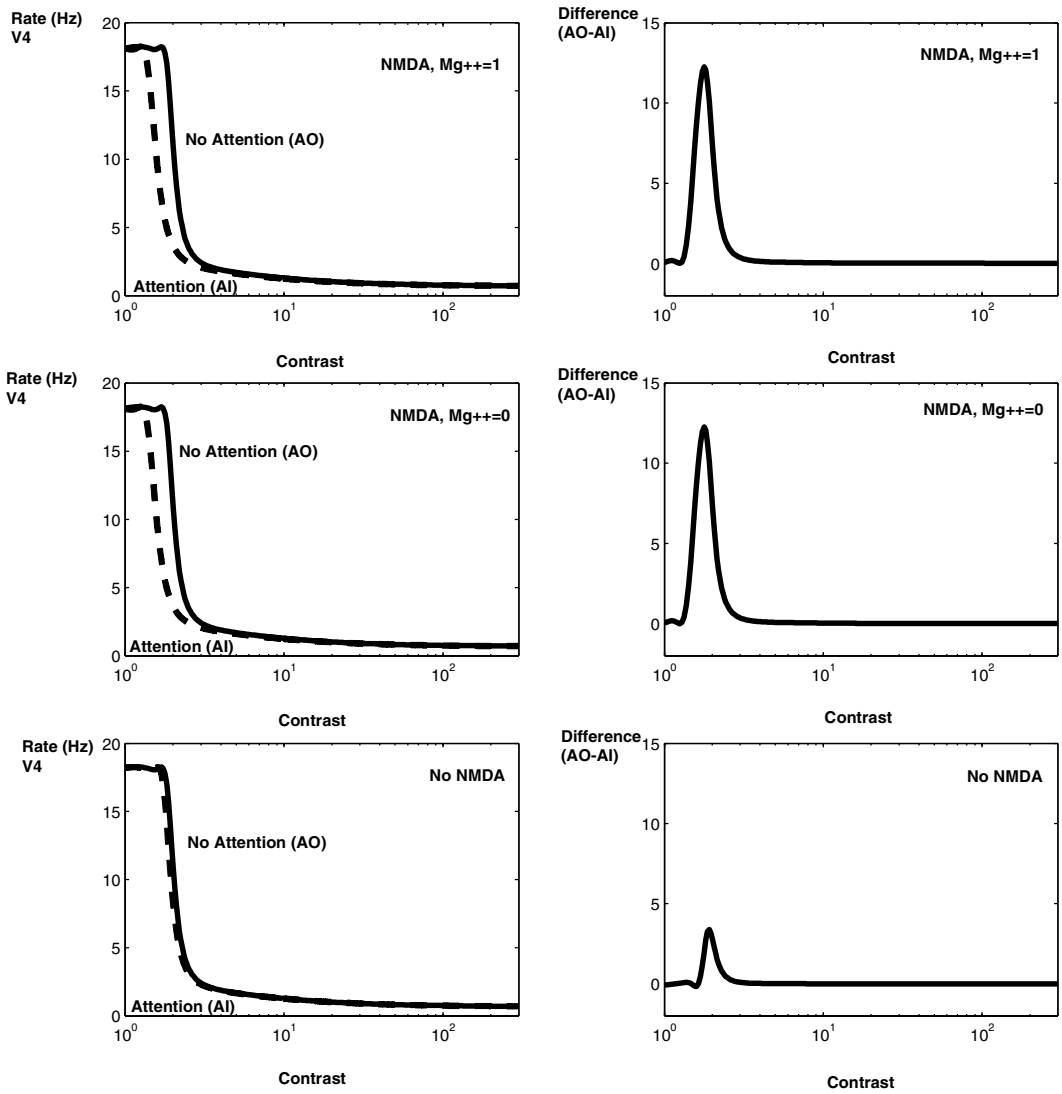

FIG. 6. *Top*: results of our simulations for the effect of interaction between contrast and attention after the design of Reynolds and Desimone (2003). *Left*: response of V4 neurons to different log contrast levels (abscissa) in the no-attention condition (AO: attending outside the receptive field) and in the attention condition (AI: attending inside the receptive field) (see legend to Fig. 5*A*). *Right*: difference between both conditions. As in the experimental observations the suppressive effect of the competing nonpreferred stimulus is higher when the contrast of that stimulus increases, but at higher levels of salience (contrast) the attentional effect disappears. *Middle*: as *top*, but with the *N*-methyl-D-aspartate (NMDA) receptor nonlinearity removed by setting $Mg^{2+} = 0$. *Bottom*: as *top*, but with the NMDA receptor time constants set to the same values as those of the AMPA receptors (see text).

Figure 7 shows the simulation results for the design of Martinez and Treue. We again found that the attentional suppressive effect implemented through $\boldsymbol{\lambda}_{att}$ of the competing nonpreferred stimulus is higher when the contrast of the preferred stimulus is at intermediate values, as in the original neurophysiological experiments. Part of the significance of this result is that the model parameters including J_f and J_b for this simulation of biased-competition effects in 2-layer networks were constrained to be those discovered to be effective based on the quantitative analyses described above of the model developed to account for the data of Reynolds et al. in V2 and V4. Thus the identical dynamical system can account quantitatively for the MT–V1 results of Martinez-Trujillo and Treue (2002) and also for the V4–V2 results of Reynolds and Desimone (2003). The results shown in Fig. 7 were replicated in further simulations when the NMDA receptors were made inactive by setting $Mg^{2+} = 0$. Thus the nonlinearity of NMDA receptors is not necessary for the gain modulation–like effects of top-down attentional bias.

In Fig. 8, we perform for the design of Reynolds and Desimone (2003) a full parameter analysis of all involved attentional modulations (enhancement and suppression in V2 and V4) by exploring the dependency of the biased competition modulation index M^{BC} as a function of the attentional bias $\boldsymbol{\lambda}_{att}$ and of the contrast of one of the stimuli (normalized so that a contrast of 1 refers to the maximum modulation). The attentional modulation effect found is maximal for intermediate levels of contrast.

Figure 5*C* shows a design associated with a prediction that can be made by setting the contrast–attention interaction study in the framework of the experimental biased competition design of Chelazzi et al. (1993) involving object attention instead of spatial attention. We measured neuronal responses from neurons in pool $S1'$ in IT (inferior temporal cortex) to a

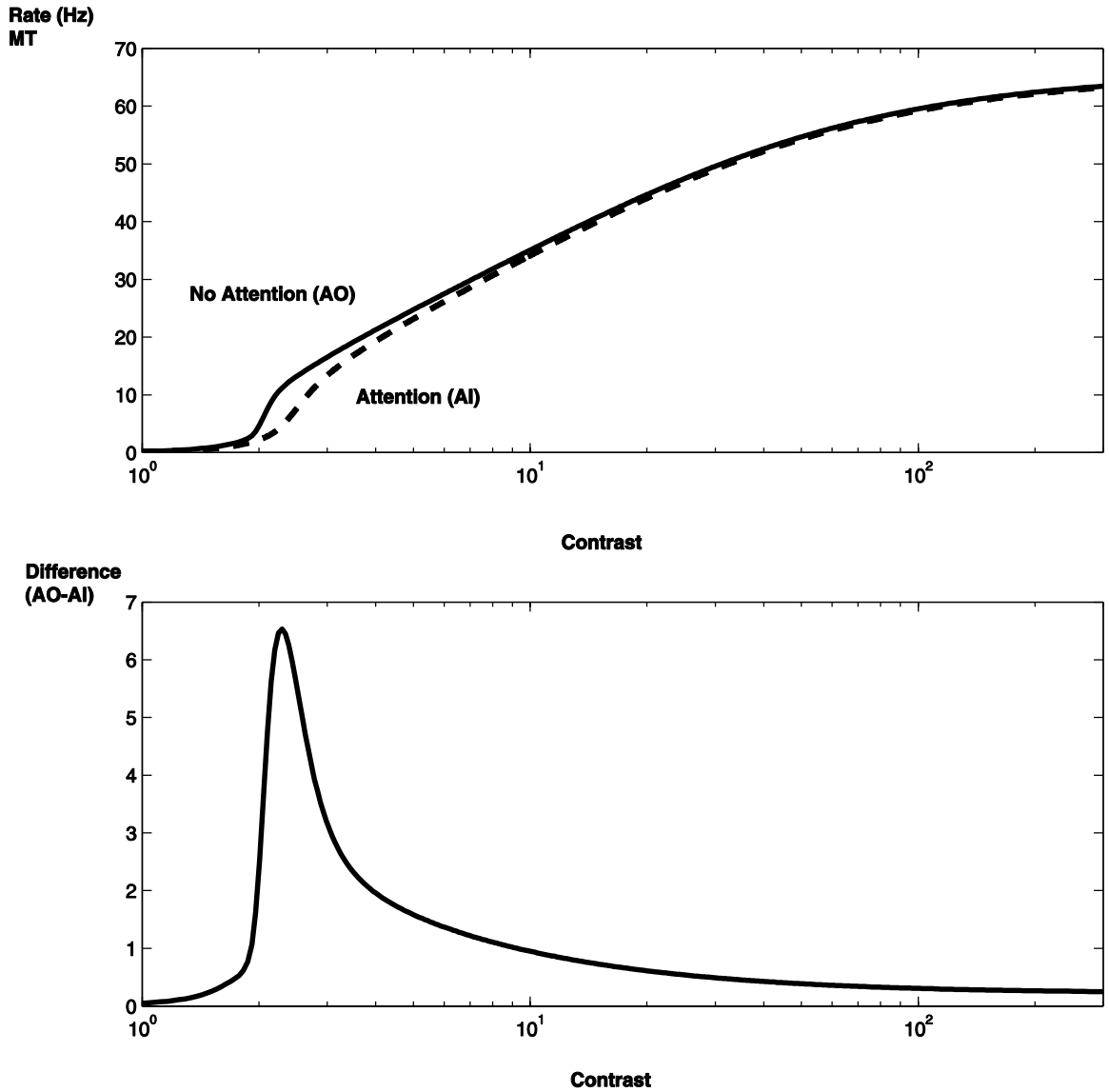

FIG. 7. Same as in Fig. 6, but for the design of Martinez and Treue (2002) (see legend to Fig. 5*B*).

preferred and a nonpreferred stimulus simultaneously presented within the receptive field. We manipulated the contrast of the stimulus that was nonpreferred for the neurons $S1'$ (in the simulation by altering $\boldsymbol{\lambda}_{\text{in}}$ to $S2$). We analyzed the effects of this manipulation for 2 conditions: without object attention or with top-down object attention on the nonpreferred stimulus $S2'$, implemented by adding an extra bias $\boldsymbol{\lambda}_{\text{att}}$ to $S2'$. The results of the simulation shown in Fig. 9 lead to the prediction that the attentional-suppressive effect implemented through $\boldsymbol{\lambda}_{\text{att}}$ on the responses of neurons $S1'$ of the competing nonpreferred stimulus ($S2$) is higher when the contrast of the nonpreferred stimulus ($S2$) is at intermediate values.

DISCUSSION

All these simulation results are consistent with neurophysiological results and show that attention has its major modulatory effect at intermediate levels of bottom-up input, and that the effect of attention disappears at low and high levels of contrast of the competing stimulus. It is important to note in Figs. 6–9 that attention in the model does have an effect like a gain change, in that the attention facilitates activity only at certain values of contrast. The important conclusion here is that in our model we were not assuming any kind of multiplicative attentional effects on the gain of neuronal responses. In our model, both attention and bottom-up input information (contrast) are implemented in the same way, by additive synaptic effects in the postsynaptic neuron. We were able to show that the nonlinearity of the NMDA receptors may facilitate nonlinear attentional effects, but is not necessary for them. Therefore we have shown that linear synaptic additivity of the bottom-up saliency effect and the top-down attentional effect is compatible not only with the biased competition dynamics but also with the interaction between (bottom-up) contrast effects and (top-down) attentional biasing. We emphasize that, although the synaptic inputs to the neuron show linear additivity, there is of course a nonlinearity in the effective activation function of the integrate-and-fire neurons, and this is what we identify as the source of the apparently multiplicative effects (Martinez-Trujillo and Treue 2002) of top-down attentional biases on

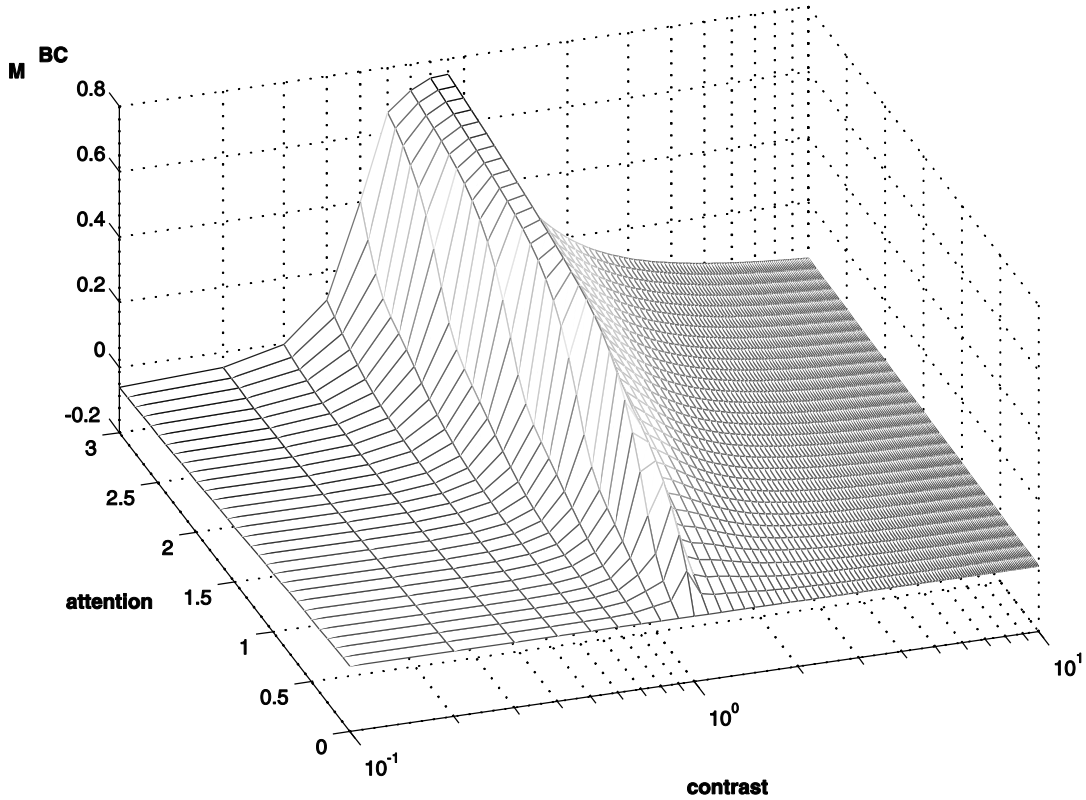

FIG. 8. Full parameter analysis of attentional modulation (enhancement and suppression in V2 and V4) for the design of Reynolds and Desimone (2003). The figure plots the biased competition modulation index M^{BC} as a function of the attentional bias $\boldsymbol{\lambda}_{att}$ and of the contrast of one of the stimuli (normalized so that contrast 1 refers to the maximum modulation).

bottom-up inputs. The relevant part of the effective activation function of the neurons (the relation between the firing and the injected excitatory currents) is the threshold nonlinearity and the first steeply rising part of the activation function, where just above threshold the firing significantly increases with small increases in synaptic inputs (cf. Amit and Brunel 1997; Brunel and Wang 2001). Attention is thus a network phenomenon that results from purely additive synaptic effects, nonlinear effects in the neurons, and cooperation–competition dynamics in the network, which together yield a variety of modulatory effects, including effects that appear (Martinez-Trujillo and Treue 2002) to be multiplicative.

The computational model we analyzed here can be used to make specific neurophysiological predictions. For example, one prediction already made relates to the contrast–attention paradigm. Instead of manipulating spatial attention as in the experimental designs considered so far in this paper, object attention in a spatial search task could be investigated using the general paradigm described by Chelazzi et al. (1993). Introducing into that paradigm extra manipulations of stimulus contrast for one of the competing stimuli (the distractor or the target in the visual search task) should also interact with object attention. The design for this prediction was specified in Fig. 5*C*, and the predictions of our computational neuroscience model are shown in Fig. 9. The results showed that, again, attentional modulation interacts maximally with the saliency of the input at intermediate contrast. This design is extremely interesting, however, because object attention interacts at the V4 level (consistent with the top-down inputs from representations of objects in the inferior temporal visual cortex; see Rolls and Deco 2002), and contrast at the V2 level, which is different from the other designs of Reynolds and Martinez where spatial attention also interacted at the V2 level.

The dynamical interplay evident in Fig. 2 and the narrow region of parameter space in which biased-competition effects are found is not intuitive at all and results from the dynamical interactions of a complex system, which can be analyzed only with the theoretical tools and with the biologically plausible and realistic modeling elements that we assumed (i.e., realistic synaptic and spiking dynamics, realistic time constants, and realistic nonlinearities). This is thus a good example of the relevance of computational neuroscience in the analysis of experimental data. For example, the results shown in Fig. 2 indicate that the feedback interarea cortical interactions (at least in the visual cortex) must be weaker (optimally by a factor of about 2.5) than the feedforward connections, which is a frequent assumption in the neurophysiological literature but not based on quantitative analysis of the dynamics.

The analyses presented here extend previous concepts of the role of biased competition in attention (Desimone and Duncan 1995; Duncan 1996; Reynolds et al. 1999; Usher and Niebur 1996) by providing the first analysis we know at the integrate-and-fire neuronal level that allows the neuronal nonlinearities in the system to be explicitly modeled, to investigate realistically the processes that underlie the apparent gain modulation effect of top-down attentional control. In the integrate-and-fire model, the competition is realized realistically by the effects of the excitatory neurons on the inhibitory neurons, and their return inhibitory synaptic connections. This is also the first integrate-and-fire analysis of top-down attentional influences in

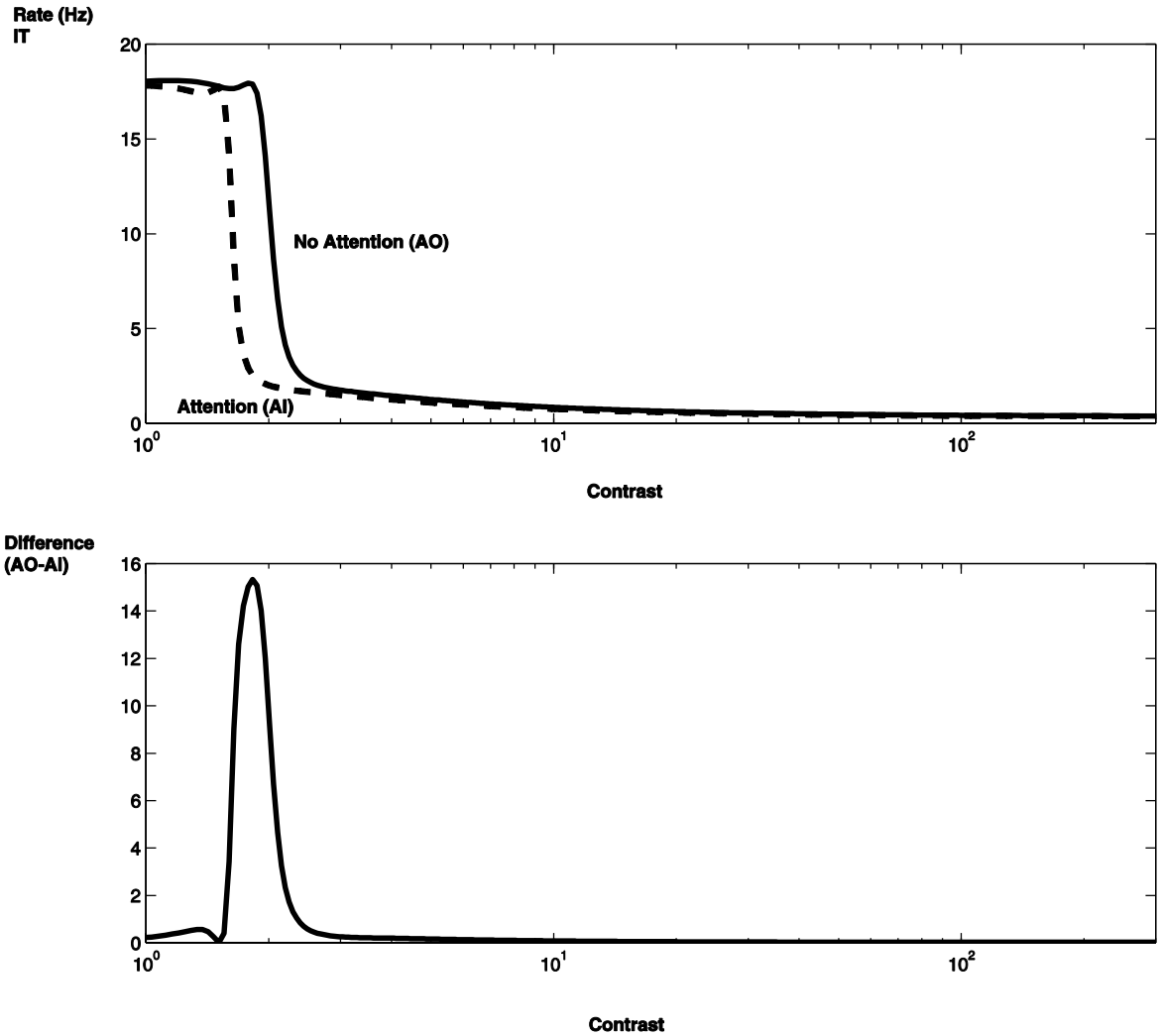

FIG. 9. Same as in Fig. 6, but for a prediction associated with the biased competition design of Chelazzi et al. (1993) involving object attention instead of spatial attention (see legend to Fig. 5*C*).

vision that explicitly models the interaction of several different brain areas (including V2, V4, IT, V3, and MT in the different simulations). Interesting earlier work by Reynolds and Desimone (1999) was based on Grossberg's shunting equations for analyzing competition and cooperation (see Grossberg 1988) and investigated feedforward saliency effects and competition. We considered top-down, biased-competition attentional effects (also considered by Spratling and Johnson 2004), but also introduced spiking neurons, synaptic dynamics, and a consistent mean-field analysis, and so were able to perform analyses of the contributions of different synaptic mechanisms and different nonlinearities in the system. The interesting work of Usher and Niebur (1996) reported model-biased competition and attention with a spiking network in a single-layer network, and we introduced here a model that has more than one layer so that the interaction between layers can be modeled, and moreover has synaptic dynamics and a mean-field analysis derived from the spiking formulation [introduced for a one-layer network by Brunel and Wang (2001)] developed for multiple-layer networks as described in APPENDIX B.

A further part of the originality and interest of the model described here is that in the form in which it can account for attentional effects in V2 and V4 in the paradigms of Reynolds et al. (1999) in the context of biased competition, the model with the same parameters effectively *makes predictions* that show that the "contrast gain" effects in MT of Martinez-Trujillo and Treue (2002) can be accounted for by the same model. In addition, the spiking model allows comparisons of the change in the spiking activity after the stimulus is presented during the transient period before the stable state of the mean field is reached. The rastergrams show simulated neuronal response onsets that are similar to those found neurophysiologically. These detailed and quantitative analyses of neuronal dynamical systems are an important step toward understanding the operation of complex processes such as top-down attention, which necessarily involve the interaction of several brain areas.

APPENDIX A

We used the mathematical formulation of integrate-and-fire (IF) neurons and synaptic currents described by Brunel and Wang (2001). Here we provide a brief summary of this framework, which we have extended to multiple interacting networks. The dynamics of the subthreshold membrane potential V of a neuron are given by the equation

$$C_m \frac{dV(t)}{dt} = -g_m[V(t) - V_L] - I_{syn}(t)$$

where C_m is the membrane capacitance taken to be 0.5 nF for excitatory neurons and 0.2 nF for inhibitory neurons; g_m is the membrane leak conductance taken to be 25 nS for excitatory neurons and 20 nS for inhibitory neurons; V_L is the resting potential of −70 mV, and I_{syn} is the synaptic current. The firing threshold is taken to be $V_{thr} = -50$ mV and the reset potential $V_{reset} = -55$ mV (see McCormick et al. 1985).

The synaptic current is given by a sum of glutamatergic, AMPA ($I_{AMPA,rec}$) and NMDA ($I_{NMDA,rec}$) mediated, recurrent excitatory currents, one AMPA ($I_{AMPA,ext}$) mediated external excitatory current, and one inhibitory GABAergic current (I_{GABA})

$$I_{syn}(t) = I_{AMPA,ext}(t) + I_{AMPA,rec}(t) + I_{NMDA,rec}(t) + I_{GABA}(t)$$

The currents are defined by

$$I_{AMPA,ext}(t) = g_{AMPA,ext}[V(t) - V_E] \sum_{j=1}^{N_{ext}} s_j^{AMPA,ext}(t)$$

$$I_{AMPA,rec}(t) = g_{AMPA,rec}[V(t) - V_E] \sum_{j=1}^{N_E} w_j s_j^{AMPA,rec}(t)$$

$$I_{NMDA,rec}(t) = \frac{g_{NMDA}[V(t) - V_E]}{1 + [Mg^{2+}]\exp[-0.062V(t)]/3.57} \times \sum_{j=1}^{N_E} w_j s_j^{NMDA}(t)$$

$$I_{GABA}(t) = g_{GABA}[V(t) - V_I] \sum_{j=1}^{N_I} s_j^{GABA}(t)$$

where $V_E = 0$ mV, $V_I = -70$ mV, and w_j are the synaptic weights; each receptor has its own fraction s_j of open channels and its own synaptic conductance g. [The external inputs to the network (attentional bias, etc.) are implemented through AMPA synapses, so that they are held constant during the simulations, allowing the functions of NMDA synapses in the internal dynamics of the network (implemented through feedforward, feedback, and internal recurrent collateral synapses) to be investigated precisely.] The NMDA synaptic current is dependent on the potential and controlled by the extracellular concentration of magnesium ($[Mg^{2+}] = 1$ mM) (Jahr and Stevens 1990). The values for the synaptic conductances for excitatory neurons are $g_{AMPA,ext} = 2.08$ nS, $g_{AMPA,rec} = 0.104$ nS, $g_{NMDA} = 0.327$ nS, and $g_{GABA} = 1.287$ nS; and for inhibitory neurons $g_{AMPA,ext} = 1.62$ nS, $g_{AMPA,rec} = 0.081$ nS, $g_{NMDA} = 0.258$ nS, and $g_{GABA} = 1.002$ nS. These values are obtained from those used by Brunel and Wang (2001) by multiplication by a factor that corrects for the difference in the number of neurons used in our model and Brunel and Wang's model. In their work the conductances were calculated so that in an unstructured network the excitatory neurons have a spontaneous spiking rate of 3 Hz and the inhibitory neurons a spontaneous rate of 9 Hz. The fractions of open channels are described by

$$\frac{ds_j^{AMPA,ext}(t)}{dt} = -\frac{s_j^{AMPA,ext}(t)}{\tau_{AMPA}} + \sum_k \delta(t - t_j^k)$$

$$\frac{ds_j^{AMPA,rec}(t)}{dt} = -\frac{s_j^{AMPA,rec}(t)}{\tau_{AMPA}} + \sum_k \delta(t - t_j^k)$$

$$\frac{ds_j^{NMDA}(t)}{dt} = -\frac{s_j^{NMDA}(t)}{\tau_{NMDA,decay}} + \alpha x_j(t)[1 - s_j^{NMDA}(t)]$$

$$\frac{dx_j(t)}{dt} = -\frac{x_j(t)}{\tau_{NMDA,rise}} + \sum_k \delta(t - t_j^k)$$

$$\frac{ds_j^{GABA}(t)}{dt} = -\frac{s_j^{GABA}(t)}{\tau_{GABA}} + \sum_k \delta(t - t_j^k)$$

where the rise time constant for NMDA synapses is $\tau_{NMDA,rise} = 2$ ms (Hestrin et al. 1990; Spruston et al. 1995), the rise time constants for AMPA and GABA are neglected because they are <1 ms, and $\alpha = 0.5$ ms^{-1}. All synapses have a delay of 0.5 ms. The decay time constant for the AMPA synapses is $\tau_{AMPA} = 2$ ms (Hestrin et al. 1990; Spruston et al. 1995), for NMDA synapses is $\tau_{NMDA,decay} = 100$ ms (Hestrin et al. 1990; Spruston et al. 1995), and for GABA synapses is $\tau_{GABA} = 10$ ms (Salin and Prince 1996; Xiang et al. 1998). The sums over k represent a sum over spikes formulated as δ-peaks [$\delta(t)$] emitted by presynaptic neuron j at time t_j^k.

We also implemented spike-frequency–adapting mechanisms, including Ca^{2+}-activated K^+ hyperpolarizing currents (Liu and Wang 2001). They assume that the intrinsic gating of K^+ afterhyperpolarizing current (I_{AHP}) is fast, and therefore its slow activation is attributed to the kinetics of the cytoplasmic Ca^{2+} concentration. This can be introduced into the model by adding an extra current term I_{AHP} in the integrate-and-fire equation, which is

$$I_{AHP} = -g_{AHP}[Ca^{2+}][V(t) - V_K]$$

where V_K is the reversal potential of the potassium channel. Furthermore, each action potential generates a small amount (α) of calcium influx, so that I_{AHP} is incremented accordingly. Between spikes the $[Ca^{2+}]$ dynamics is modeled as a leaky integrator with a decay constant τ_{Ca}. Thus the calcium dynamics can be described by the following system of equations

$$\frac{d[Ca^{2+}]}{dt} = -\frac{[Ca^{2+}]}{\tau_{Ca}} \tag{A1}$$

$$\text{If } V(t) = V_{thr}, \quad \text{then } [Ca^{2+}] = [Ca^{2+}] + \alpha, \quad \text{and} \quad V = V_{reset} \tag{A2}$$

which are coupled to the above-mentioned modified equations of this APPENDIX. The $[Ca^{2+}]$ is initially set to be 0 μM, $\tau_{Ca} = 600$ ms, $\alpha = 0.005$, $V_K = -80$ mV, and $g_{AHP} = 7.5$ nS (see Liu and Wang 2001).

APPENDIX B

The mean-field approximation used in the present work was derived by Brunel and Wang (2001), assuming that the network of integrate-and-fire neurons is in a stationary state. We extended the results to include spike-frequency–adapting mechanisms, based on Ca^{2+}-activated K^+ hyperpolarizing currents, as described in APPENDIX A. In this formulation the potential of a neuron is calculated as

$$\tau_x \frac{dV(t)}{dt} = -V(t) + \mu_x + \sigma_x \sqrt{\tau_x}\eta(t)$$

where $V(t)$ is the membrane potential, x labels the populations, τ_x is the effective membrane time constant, μ_x is the mean value the membrane potential would have in the absence of spiking and fluctuations, σ_x measures the magnitude of the fluctuations, and η is a Gaussian process with absolute exponentially decaying correlation function with time constant τ_{AMPA}. The quantities μ_x and σ_x^2 are given by

$$\mu_x = \frac{(T_{ext}\nu_{ext} + T_{AMPA}n_x + \rho_1 N_x)V_E + \rho_2 N_x\langle V\rangle + T_I w_{I,x}\nu_I V_I + V_L + \dfrac{g_{AHP}[Ca^{2+}]_x V_K}{g_m}}{S_x}$$

$$\sigma_x^2 = \frac{(g_{AMPA,ext}^2\nu_{ext} + g_{AMPA,rec}^2\nu_x)(\langle V\rangle - V_E)^2\tau_{AMPA}^2\tau_x}{g_m^2\tau_m^2}$$

where $w_{I,x}$ represents the weights from the inhibitory neurons to the pool x, $[Ca^{2+}]_x$ is the population-averaged cytoplasmic concentration of Ca^{2+} in neurons in pool x, ν_{ext} is the external impinging spiking rate (including spontaneous activity and eventually external stimuli or

attentional bias), ν_I is the population-averaged spiking rate of the inhibitory pool,[1] $\tau_m = C_m/g_m$ with the values for the excitatory or inhibitory neurons depending of the pool considered and the other quantities are given by

$$S_x = 1 + T_{ext}\nu_{ext} + T_{AMPA}n_x + (\rho_1 + \rho_2)N_x + T_I w_{I,x}\nu_I + \frac{g_{AHP}[Ca^{2+}]_x}{g_m}$$

$$\tau_x = \frac{C_m}{g_m S_x}$$

$$n_x = \sum_{j=1}^{p} f_j w_{j,x}\nu_j$$

$$N_x = \sum_{j=1}^{p} f_j w_{j,x}\psi(\nu_j)$$

$$\psi(\nu) = \frac{\nu\tau_{NMDA}}{1 + \nu\tau_{NMDA}}\left[1 + \frac{1}{1 + \nu\tau_{NMDA}}\sum_{n=1}^{\infty}\frac{(-\alpha\tau_{NMDA,rise})^n T_n(\nu)}{(n+1)!}\right]$$

$$T_n(\nu) = \sum_{k=0}^{n}(-1)^k\binom{n}{k}\frac{\tau_{NMDA,rise}(1 + \nu\tau_{NMDA})}{\tau_{NMDA,rise}(1 + \nu\tau_{NMDA}) + k\tau_{NMDA,decay}}$$

$$\tau_{NMDA} = \alpha\tau_{NMDA,rise}\tau_{NMDA,decay}$$

$$T_{ext} = \frac{g_{AMPA,ext}\tau_{AMPA}}{g_m}$$

$$T_{AMPA} = \frac{g_{AMPA,rec}N_E\tau_{AMPA}}{g_m}$$

$$\rho_1 = \frac{g_{NMDA}N_E}{g_m J}$$

$$\rho_2 = \beta\frac{g_{NMDA}N_E(\langle V_x\rangle - V_E)(J-1)}{g_m J^2}$$

$$J = 1 + \gamma\exp(-\beta\langle V_x\rangle)$$

$$T_I = \frac{g_{GABA}N_I\tau_{GABA}}{g_m}$$

$$\langle V_x\rangle = \mu_x - (V_{thr} - V_{reset})\nu_x\tau_x \qquad \text{(B1)}$$

where p is the number of excitatory pools, f_x is the fraction of neurons in the excitatory x pool, $w_{j,x}$ is the weight of the connections from pool x to pool j, ν_x is the population-averaged spiking rate of the x excitatory pool, $\gamma = [Mg^{2+}]/3.57$, $\beta = 0.062$, and the average membrane potential $\langle V_x\rangle$ has a value between −55 and −50 mV.

The spiking rate of a pool as a function of the defined quantities is then given by

$$\nu_x = \phi(\mu_x, \sigma_x) \qquad \text{(B2)}$$

where

$$\phi(\mu_x, \sigma_x) = \left\{\tau_{rp} + \tau_x\int_{\beta(\mu_x,\sigma_x)}^{\alpha(\mu_x,\sigma_x)} du\,\sqrt{\pi}\exp(u^2)[1 + \mathrm{erf}(u)]\right\}^{-1}$$

$$\alpha(\mu_x, \sigma_x) = \frac{(V_{thr} - \mu_x)}{\sigma_x}\left(1 + 0.5\frac{\tau_{AMPA}}{\tau_x}\right) + 1.03\sqrt{\frac{\tau_{AMPA}}{\tau_x}} - 0.5\frac{\tau_{AMPA}}{\tau_x}$$

$$\beta(\mu_x, \sigma_x) = \frac{(V_{reset} - \mu_x)}{\sigma_x}$$

with erf (u) is the error function and τ_{rp} is the refractory period, which is considered to be 2 ms for excitatory neurons and 1 ms for inhibitory neurons. To solve the system of equations defined by *Eq. B2* for all values of x we numerically integrate *Eq. B1* and the differential equation below, describing a *fake dynamics* of the system, which has fixed-point solutions corresponding to *Eq. B2*

$$\tau_x\frac{d\nu_x}{dt} = -\nu_x + \phi(\mu_x, \sigma_x) \qquad \text{(B3)}$$

In parallel we update the dynamics of $[Ca^{2+}]_x$ by assuming an adiabatic approximation on the dynamical *Eqs. A1* and *A2*, that is

$$\tau_{Ca}\frac{d[Ca^{2+}]_x}{dt} = -[Ca^{2+}]_x + \alpha\tau_{Ca}\nu_x \qquad \text{(B4)}$$

APPENDIX C

Herein we describe how the simulations corresponding to the mean-field explorations and the explicit spiking dynamics of the network were performed. For all simulation periods studied, the mean-field *Eqs. B1* and *B3* were integrated using the Euler method with step size 0.1 and 8,000 iterations, which always allowed for convergence. All excitatory pools were initialized with a frequency of 3 Hz and the inhibitory pools with 9 Hz. These values correspond to the approximate values of the attractors for the 2 types of pools when the network is not driven by stimulus-specific inputs, but instead just driven by the background spontaneous activity. During all simulations both specific pools *S*1 and *S*2 of the lower layer (V2) received an extra bias λ_{in} = 250 Hz input, coding both visual stimuli presented simultaneously. In the simulations requiring spatial attention, the pool corresponding to the attended location (associated with *S*1 or *S*2 in layer V2) received an extra bias λ_{att} = 10 Hz. In the simulations requiring object attention, the pool corresponding to the attended stimulus (associated with *S*1′ or *S*2′in layer V4) received an extra bias λ_{att} = 10 Hz.

The simulations of the spiking dynamics of the network were done for both array and cue trials. The equations presented in APPENDIX A were integrated numerically using the second-order Runge–Kutta method with step size 0.05 ms. Each simulation was started by a period of 100 ms where no stimulus was presented, to allow the network to stabilize. This period was followed by a sequence composed of the presentation of both stimuli lasting 250 ms and in some conditions including an attentional bias, and followed again by a period of 250 ms where no stimulus was presented, as in the experimental paradigm. The nonstationary evolution of spiking activity is averaged over 20 trials initialized with different random seeds.

APPENDIX D

In this APPENDIX we bring together the fixed parameters of the model in Table D1, and then provide information about the values of further parameters used in the simulations, and how well the simulations fit the experimental data.

The optimal values of additional parameters used in the simulations shown in Figs. 2, 3, 4, and 6 of the experiment of Reynolds et al. (1999), and in Fig. 9, were as follows: $J_f = 1.6$, $J_b = 0.5$, $K_f = 0.15$, $K_b = 0.06$, $c = 0.1$, and $M^{BC} = 0.92$. These led to the following best fits: $M^{S1} = 0.109$, $M^{S1'} = 0.29$, $M^{S2} = 0.072$, and $M^{S2'} = 0.22$, which can be compared with the experimental values of $M^{S1} = 0.1$, $M^{S1'} = 0.3$, $M^{S2} = 0.08$, and $M^{S2'} = 0.25$.

The optimal values of the additional parameters used in the simulations shown in Fig. 7 of the experiment of Martinez-Trujillo and Treue (2002) were as follows: $J_f = 1.45$, $J_b = 0.45$, $K_f = 0.1125$, $K_b = 0.045$, $c = 0.075$, and $M^{BC} = 0.85$. These led to the following

[1] In our architecture we have 2 inhibitory pools, I (for V2) and I′ (for V4). Thus in these equations one has to use one or the other inhibitory pool according to where the pool x is. That is, if x belongs to layer V2, $w_{I,x}$ and ν_I correspond to the inhibitory pool I; if x belongs to layer V4, one has to use instead $w_{I',x}$ and $\nu_{I'}$, which correspond to the inhibitory pool I′.

TABLE D1. *Default parameters used in the integrate-and-fire simulations*

Parameter	Value	Parameter	Value
N_E	800	V_I	−70 mV
N_I	200	$g_{AMPA,ext}$ (excitatory)	2.08 nS
f	0.1	$g_{AMPA,rec}$ (excitatory)	0.104 nS
w_+	1.5	g_{NMDA} (excitatory)	0.327 nS
w	1.0	g_{GABA} (excitatory)	1.287 nS
w_I	1.0	$g_{AMPA,ext}$ (inhibitory)	1.62 nS
w_I'	1.25	$g_{AMPA,rec}$ (inhibitory)	0.081 nS
N_{ext}	800	g_{NMDA} (inhibitory)	0.258 nS
$\boldsymbol{\nu}_{ext}$	2.4 kHz	g_{GABA} (inhibitory)	1.002 nS
$\boldsymbol{\lambda}_{in}$	250 Hz	$\boldsymbol{\tau}_{NMDA,decay}$	100 ms
$\boldsymbol{\lambda}_{att}$	10 Hz	$\boldsymbol{\tau}_{NMDA,rise}$	2 ms
C_m (excitatory)	0.5 nF	$\boldsymbol{\tau}_{AMPA}$	2 ms
C_m (inhibitory)	0.2 nF	$\boldsymbol{\tau}_{GABA}$	10 ms
g_m (excitatory)	25 nS	$\boldsymbol{\alpha}$	0.5 ms^{-1}
g_m (inhibitory)	20 nS	$[Ca^{2+}]$	0 μM
V_L	−70 mV	$\boldsymbol{\tau}_{Ca}$	600 ms
V_{thr}	−50 mV	V_K	−80 mV
V_{reset}	−55 mV	g_{AHP}	7.5 nS
V_E	0 mV		

best fits: $M^{S1} = 0.12$, $M^{S1'} = 0.37$, $M^{S2} = 0.076$, and $M^{S2'} = 0.26$, which can be compared with the experimental values of $M^{S1} = 0.1$, $M^{S1'} = 0.3$, $M^{S2} = 0.08$, and $M^{S2'} = 0.25$ [which, because Martinez-Trujillo and Treue (2002) did not measure these directly, are estimates based on what was found by Reynolds et al. (1999)]. [Parameter c was slightly smaller in the simulations of the experiment of Martinez-Trujillo and Treue (2002) because they used opposite directions of movement as the 2 stimuli, whereas Reynolds et al. (1999) used 2 orientations that are more similar as stimuli.]

GRANTS

This work was supported by the German Ministry of Research, Federal Ministry of Education & Research Grant 01IBC01A, and by the Medical Research Council. G. Deco was supported by Institució Catalana de Recerca i Estudis Avançats.

REFERENCES

Abeles A. *Corticonics*. New York: Cambridge Univ. Press, 1991.

Amit D and Brunel N. Model of global spontaneous activity and local structured activity during delay periods in the cerebral cortex. *Cereb Cortex* 7: 237–252, 1997.

Brunel N and Wang X. Effects of neuromodulation in a cortical networks model of object working memory dominated by recurrent inhibition. *J Comput Neurosci* 11: 63–85, 2001.

Chelazzi L. Serial attention mechanisms in visual search: a critical look at the evidence. *Psychol Res* 62: 195–219, 1998.

Chelazzi L, Miller E, Duncan J, and Desimone R. A neural basis for visual search in inferior temporal cortex. *Nature* 363: 345–347, 1993.

Connor CE, Preddie D, Gallant JL, and Van Essen D. Spatial attention effects in macaque area V4. *J Neurosci* 17: 3201–3214, 1997.

Corchs S and Deco G. Large-scale neural model for visual attention: integration of experimental single cell and fMRI data. *Cereb Cortex* 12: 339–348, 2002.

Corchs S and Deco G. Feature-based attention in human visual cortex: simulation of fMRI data. *Neuroimage* 21: 36–45, 2004.

Deco G and Lee TS. A unified model of spatial and object attention based on inter-cortical biased competition. *Neurocomputing* 44–46: 775–781, 2002.

Deco G, Pollatos O, and Zihl J. The time course of selective visual attention: theory and experiments. *Vision Res* 42: 2925–2945, 2002.

Deco G and Rolls ET. Object-based visual neglect: a computational hypothesis. *Eur J Neurosci* 16: 1994–2000, 2002.

Deco G and Rolls ET. Attention and working memory: a dynamical model of neuronal activity in the prefrontal cortex. *Eur J Neurosci* 18: 2374–2390, 2003.

Deco G and Rolls ET. A neurodynamical cortical model of visual attention and invariant object recognition. *Vision Res* 44: 621–644, 2004.

Deco G, Rolls ET, and Horwitz B. "What " and "where " in visual working memory: a computational neurodynamical perspective for integrating fMRI and single-neuron data. *J Cogn Neurosci* 16: 683–701, 2004.

Deco G and Zihl J. Top-down selective visual attention: a neurodynamical approach. *Vis Cogn* 8: 119–140, 2001.

Del Giudice P, Fusi S, and Mattia M. Modeling the formation of working memory with networks of integrate-and-fire neurons connected by plastic synapses. *J Physiol* (*Paris*) 97: 659–681, 2003.

Desimone R and Duncan J. Neural mechanisms of selective visual attention. *Annu Rev Neurosci* 18: 193–222, 1995.

Duncan J. Cooperating brain systems in selective perception and action. In: *Attention and Performance XVI*, edited by Inui T and McClelland JL. Cambridge, MA: MIT Press, 1996, p. 549–578.

Duncan J and Humphreys G. Visual search and stimulus similarity. *Psychol Rev* 96: 433–458, 1989.

Grossberg S. Nonlinear neural networks: principles, mechanisms, and architectures. *Neural Networks* 1: 17–61, 1988.

Heinke D, Deco G, Zihl J, and Humphreys G. A computational neuroscience account of visual neglect. *Neurocomputing* 44–46: 811–816, 2002.

Hestrin S, Sah P, and Nicoll R. Mechanisms generating the time course of dual component excitatory synaptic currents recorded in hippocampal slices. *Neuron* 5: 247–253, 1990.

Jahr C and Stevens C. Voltage dependence of NMDA-activated macroscopic conduntances predicted by single-channel kinetics. *J Neurosci* 10: 3178–3182, 1990.

Kastner S, De Weerd P, Desimone R, and Ungerleider L. Mechanisms of directed attention in the human extrastriate cortex as revealed by functional MRI. *Science* 282: 108–111, 1998.

Kastner S, Pinsk M, De Weerd P, Desimone R, and Ungerleider L. Increased activity in human visual cortex during directed attention in the absence of visual stimulation. *Neuron* 22: 751–761, 1999.

Liu Y and Wang X-J. Spike-frequency adaptation of a generalized leaky integrate-and-fire model neuron. *J Comput Neurosci* 10: 25–45, 2001.

Luck S, Chelazzi L, Hillyard S, and Desimone R. Neural mechanisms of spatial selective attention in areas V1, V2, and V4 of macaque visual cortex. *J Neurophysiol* 77: 24–42, 1997.

Martinez-Trujillo J and Treue S. Attentional modulation strength in cortical area MT depends on stimulus contrast. *Neuron* 35: 365–370, 2002.

McCormick D, Connors B, Lighthall J, and Prince D. Comparative electrophysiology of pyramidal and sparsely spiny stellate neurons in the neocortex. *J Neurophysiol* 54: 782–806, 1985.

Miller E, Gochin P, and Gross C. Suppression of visual responses of neurons in inferior temporal cortex of the awake macaque by addition of a second stimulus. *Brain Res* 616: 25–29, 1993.

Moran J and Desimone R. Selective attention gates visual processing in the extrastriate cortex. *Science* 229: 782–784, 1985.

Motter B. Focal attention produces spatially selective processing in visual cortical areas V1, V2, and V4 in the presence of competing stimuli. *J Neurophysiol* 70: 909–919, 1993.

Motter B. Neural correlates of attentive selection for colours or luminance in extrastriate area V4. *J Neurosci* 14: 2178–2189, 1994.

Reynolds J and Desimone R. The role of neural mechanisms of attention in solving the binding problem. *Neuron* 24: 19–29, 1999.

Reynolds J and Desimone R. Interacting roles of attention and visual saliency in V4. *Neuron* 37: 853–863, 2003.

Reynolds J, Chelazzi L, and Desimone R. Competitive mechanisms subserve attention in macaque areas V2 and V4. *J Neurosci* 19: 1736–1753, 1999.

Rolls ET and Deco G. *Computational Neuroscience of Vision*. Oxford, UK: Oxford Univ. Press, 2002.

Rolls ET and Treves A. *Neural Networks and Brain Function*. Oxford, UK: Oxford Univ. Press, 1998.

Salin P and Prince D. Spontaneous GABA-A receptor mediated inhibitory currents in adult rat somatosensory cortex. *J Neurophysiol* 75: 1573–1588, 1996.

Sato T. Interactions of visual stimuli in the receptive fields of inferior temporal neurons in awake macaques. *Exp Brain Res* 77: 23–30, 1989.

Spitzer H, Desimone R, and Moran J. Increased attention enhances both behavioral and neuronal performance. *Science* 240: 338–340, 1988.

Spratling MW and Johnson MH. A feedback model of visual attention. *J Cogn Neurosci* 16: 219–237, 2004.

Spruston N, Jonas P, and Sakmann B. Dendritic glutamate receptor channel in rat hippocampal CA3 and CA1 pyramidal neurons. *J Physiol* 482: 325–352, 1995.

Szabo M, Almeida R, Deco G, and Stetter M. Cooperation and biased competition model can explain attentional filtering in the prefrontal cortex. *Eur J Neurosci* 19: 1969–1977, 2004.

Tuckwell H. *Introduction to Theoretical Neurobiology*. Cambridge, UK: Cambridge Univ. Press, 1988.

Usher M and Niebur E. Modelling the temporal dynamics of IT neurons in visual search: a mechanism for top-down selective attention. *J Cogn Neurosci* 8: 311–327, 1996.

Wilson FAW, O'Scalaidhe SP, and Goldman-Rakic P. Functional synergism between putative gamma-aminobutyrate-containing neurons and pyramidal neurons in prefrontal cortex. *Proc Natl Acad Sci USA* 91: 4009–4013, 1994.

Xiang Z, Huguenard J, and Prince D. GABA-A receptor mediated currents in interneurons and pyramidal cells of rat visual cortex. *J Physiol* 506: 715–730, 1998.